# Performance Measures of Direct Metal Laser Sintering Hybrid Milling: Mechanical Properties and Environmental Performance Indicators

A THESIS

Presented in partial fulfillment of the requirement for the Master of Science in Mechanical Engineering

University of Minnesota Duluth

By

Nabeel Ahmad

Advisor

Dr. Emmanuel Enemuoh

July 2019

# Thesis Committee Members

- Emmanuel Enemuoh (eenemuoh@umn.edu) - Primary adviser, Chair, Reviewer
- Michael Greminger (mgreming@umn.edu) - Reviewer
- Manik Barman (mbarman@umn.edu) - Reviewer

## Acknowledgement

I am extremely thankful to my advisor Dr. Enemuoh who, in addition to providing technical support and guidance, gave me independence and flexibility to carry out this thesis work. Also, I would like to thank Dr. Greminger and Dr. Barman from University of Minnesota, Duluth for reviewing thesis and serving in defense committee. Moreover, thanks to Dr. Muhammad Imran from Tabuk University for his generous assistance and helpful comments. Also, my sincere gratitude to all colleagues of MSME especially Irfan Tahir and my mentor Zahra Navabi who were great source of inspiration and moral support for me.

# Executive Summary

Applications of metal additive manufacturing (AM) has increased substantially because it allows cost and resources efficient small-scale production required in industries such as aerospace and mold and die manufacturing. Geometric and dimensional accuracy of parts produced by AM is still subpar compared to conventional subtractive approaches. Recently, hybrid additive-subtractive called direct metal laser sintering hybrid milling (DMLS-HM) technology has been introduced which combines strengths and robustness of both additive and subtractive units. This thesis explores the adoption consequences and impacts of DMLS-HM through relative performance measures of mechanical and metallurgical properties as well as environmental impact assessment. This was achieved by first characterizing mechanical properties of Maraging steel powder and comparing it with conventional DMLS to understand the degree of variability. It was found out that DMLS-HM has superior mechanical properties for impact toughness and surface finish; however, tensile strength and hardness values were similar with DMLS. Environmental performance assessment was achieved by first identifying and finding the energy requirements in subsystems (additive and subtractive) of DMLS-HM and then converting into equivalent carbon emission. Carbon emission results for DMLS-HM printed geometry were compared with two other manufacturing approaches namely electron beam melting and conventional milling which fabricated the same geometry. The DMLS-HM process showed higher energy consumption during the part production stage with an average 84% more than EBM and CM processes. However, the CM was dominant in energy consumption during the procurement stage with an around 70% more energy than DMLS-HM and EBM processes. The outcome of this research project will contribute to the understanding of basic physics of energy consumption in AM and can be used in suitable process selection and setting sustainable manufacturing goals.

# Table of Contents

# List of Tables

# List of Figures

# CHAPTER 1

# INTRODUCTION AND RESEARCH BACKGROUND

## 1.1 Overview of Additive Manufacturing (AM)

Additive Manufacturing (AM) is defined by American Society for Testing and Materials (ASTM) as the "process of joining materials to make objects from 3D model data usually layer upon layer, as opposed to subtractive manufacturing technologies such as traditional machining" [1]. In a typical AM process, a designer develops a CAD model to be made, which is then converted into surface tessellation (STL) file. STL file is then imported into machine computer, where the digital information of CAD file is sliced into horizontal layers of specified thickness by the computer software. AM system then builds these layers with each new layer coming over the top of previous layer.

AM system is inherently diverse; it has ability to print metals, polymers and ceramics. Depending on requirements and type of material, AM fuses base material and builds layer by layer and forms the desired shape geometry. This means, there is no need to make customized tooling unlike subtractive and formative manufacturing processes in which molds or special machine tools are necessitated. Moreover, nature of AM processes results into little or no waste. Because of such inherent manufacturing capabilities, AM technology has caught attention of industries and researchers alike. Initially, AM was used to make prototype for aesthetical designs of architecture and product prototypes because of cost effectiveness and its excellent capability of rapid prototyping, but the technology advanced rapidly, and applications have widened into mold industry, medical, sculpture, architecture, manufacturing industry and many other areas.

AM technique foresees a new revolution in manufacturing industry; however, there is still long way to go before harnessing its full potential. Scalability and final part quality remain big concern. Poor surface finish of final parts limits the practical use and often post processing operations are required. Therefore, over the years there has been

consistent effort to “redefine, reimagine and innovate” the current understanding. One can imagine the height of research by amount of funding being awarded towards AM research. Weber et al.[2] detailed analysis of major breakthroughs of AM and amount of NSF funding (240 million dollars) awarded for AM research. Big corporations such as General Electric (GE) is investing and doing intensive research in metal AM for making functional parts. If successful, GE would be able to reduce lead time, refine and simplify manufacturing supply chain by getting independence from third party manufacturers and will improve performance and useful life of final parts. AM has also gained popularity because of its ability to produce mass customization of products. Mass customization is particularly useful in biomedical field where patients are required to have tailored-made organs. Trend of customization is catching more attention in functional products and Wohler Associates [3] predicted that around 50% of commercial products will be manufactured using 3D printing in 2020. In short, AM is poised to become the foundation of fourth industrial revolution because of its flexibility, allowing the manufacturing of almost any geometry irrespective of complexity, ability to reduce cost and lead time and encouraging autonomous and decentralized manufacturing operations.

## 1.2 Benefits of AM over Traditional Manufacturing

AM is still evolving, and work is being done in creating new efficient methods of manufacturing process and product design. Thus, it is giving hope to industries who are aiming to improve manufacturing efficiency. It is anticipated that AM will transcend the traditional manufacturing process and is set to become norm in few decades to come. There are five potential benefits of AM over traditional manufacturing: cost, speed, mass customization, reduced waste and little to no skill. Table 1 gives the detailed overview of benefits of AM vs traditional manufacturing[4].

**Table 1 AM Benefits over Traditional Manufacturing [4]**

| Application Area | Advantages |
|---|---|
| Spare Parts Production | Reduce labor cost, repair time |
| Small scale batch production | Cost efficient production, no costs associated with tooling |
| Customized items | Mass customization at lower cost |
| Complex parts | Can fabricate complex parts at lower cost |
| Complex work-piece | Can generate complex workpiece |
| Rapid Manufacturing | Direct manufacturing |
| Part consolidation | Ability to build parts as a whole<br>Reduces sub-assembly units |
| Rapid Prototyping | Reduce market time and product development cost |

## 1.3 Barriers and Challenges of AM

**Mass Manufacturing**: Present technological level of AM offers the ability to fabricate parts with low volume production and increased geometric complexity. However, large scale batch production of parts using AM is still not economically viable and injection molding takes the lead and is more cost effective than AM [5]. In short, economy of scale of AM remains a concern to address.

**Build Time and Layer Thickness:** Layer resolution and scalability have inherent tradeoffs between each other. Greater layer thickness (Low layer resolution) will increase the scalability of printed parts and decrease the overall build time. However, this will in turn drastically reduce the finishing of final parts.

**Material Choice**: Since AM is still in its nascent phase, it is evident that limited material selection is available in market. Those raw water atomized metal powdered form that are available in markets are of poorer quality; as a result, printed parts suffer from anisotropic mechanical properties due to poor interlayer bonding. Moreover, most AM

systems process only a single type of material, so a product with multi-variety mechanical properties that renders different functionalities is difficult to fabricate.

**Intellectual property and Standardization:** The ability to print a CAD model without elaborate tool design and skillset with the help of AM has made it easier for almost everyone to print whatever one wants. This new development has created a new challenge for investors, designers and manufacturers. The ability to download open source files and then print is a form of infringement that needs to be resolved to protect the stakes of investors.

Moreover, AM systems need to be standardized to enhance efficiency of production operation and repeatability of fabricated parts. With the presence of wide range of AM machine types and systems, it is high time that organizations such as ASTM develop standard material, process, test standards, calibration as well as file format standards for AM industry.

## 1.4 Introduction of Metal AM

Metal AM is generally categorized into two main groups: Powder Bed fusion (PBF) and Directed Energy Deposition (DED). As per ASTM/International Organization for Standardization (ISO) terminology[6] “DED is an additive manufacturing process in which focused thermal energy is used to fuse materials as they are being deposited.” Generally, raw material is either in form of metal powder or wire while being deposited. DED is broadly used in maintaining and fixing structural parts. Figure 1 illustrates the working principles of DED.

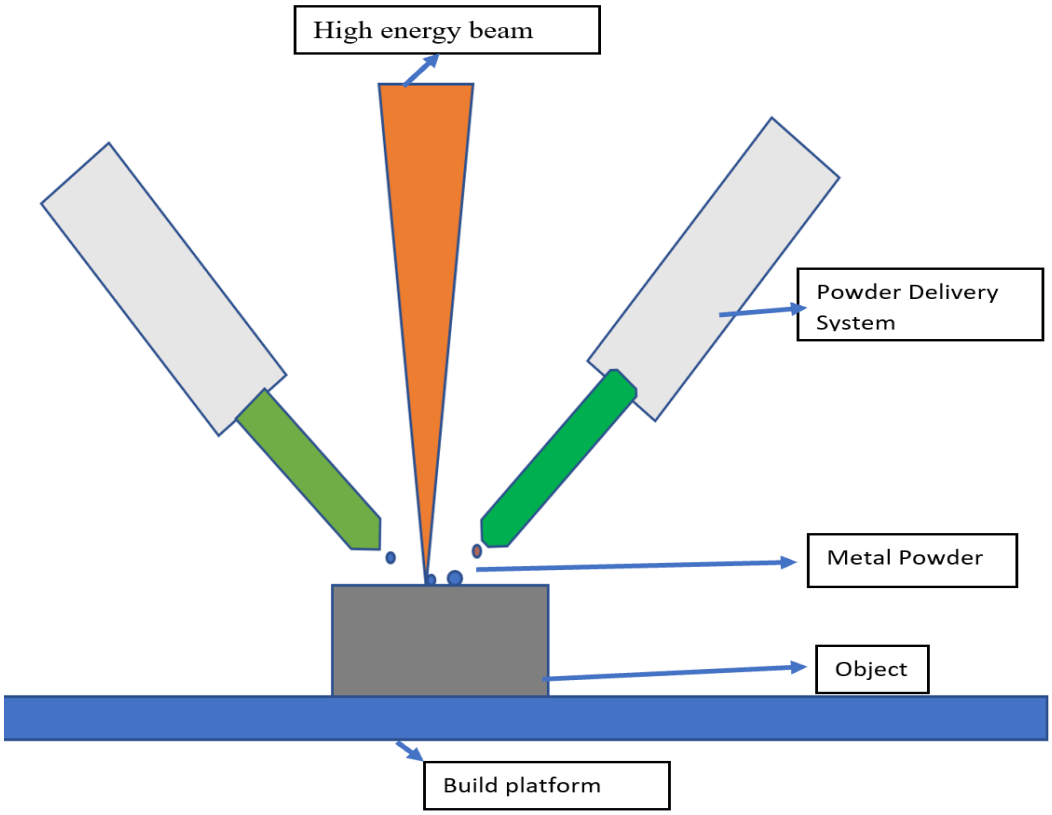


**Figure 1 Directed Energy Deposition Process Schematics[7]**

**Powder bed fusion (PBF)** is one of important technologies because of its ability to fabricate small volume and complex metallic function parts. It involves the process of building material from thin layers of very fine powder bonded together layer by layer over the top of preceding layer. This succession of layers is fused together by thermal energy until a fully 3D part is realized. Excess powder is either removed by vacuum or used sometimes for postprocessing such as sintering, coating or filtering. Direct metal laser sintering, electron beam melting and selective laser melting are common metal PBF techniques. Figure 2 illustrates the working principle of PBF system.

PBF can be further categorized by the type of energy sources used. If regions of the powder are selectively being fused using laser, this would lie in category of Selective Laser Sintering (SLS) or Selective Laser Melting. In SLS process, laser scan partially melts the powder and fuse them together. The high temperature in the proximity of grain's surface helps fusing powder at the molecular levels [9]. It is typically used for low

melting alloys of aluminum and polymers. The term direct metal laser sintering (DMLS) is especially used for metals. In SLM, material is completely melted using laser to achieve superior mechanical properties. Physics of EBM process is similar in nature except the thermal energy source is electron beam.

This technology can be integrated with conventional machining to exploit the strengths of metal PBF and traditional machining. Direct metal laser sintering hybrid milling (DMLS-HM) is one such technology which utilizes design flexibility of AM and precision of cutting operations.

## 1.5 Direct Metal Laser Sintering Hybrid Milling Process

Matsuura LUMEX 25 machine was used in manufacturing the test samples. LUMEX is a single machine platform integrating a fiber laser for state-of-the-art metal sintering in a 256mm by 256mm by 300mm space and a machining center for performing high accuracy, high speed milling. The process comprises of three main phases: squeezing, laser sintering and milling. Squeezing is performed by laminating metal powder to a specified thickness (typically 0.01- 0.1 mm) on the base plate located on the table as illustrated in Figure 3. Then a 400 watts high efficient Yb fiber laser of high beam quality is used to sinter the metal powder into the desired product shape bonded to the processing table. The upper surface of the table is heated to mitigate rapid temperature changes resulting from laser sintering, therefore, increasing the sintering precision. After the metal powder is sintered, the LUMEX squeezes and supplies metal powder with a prescribed thickness to form the next layer and sinter all the laminated layers. Squeezing and laser sintering steps are repeated 10 times, then, the LUMEX goes to the phase of milling as illustrated with Figure 3. An end mill incorporating oil-air lubricated spindle with high spindle speed and a 1/10 taper special BT20 tool shank performs milling of the contour of the part precisely to a finish. The LUMEX 25 repeats the sintering and milling of the part to build from the bottom layer to top layers, irrespective of the complexity of the internal shape. Samples were built vertically along z-direction as shown in the figure 4.

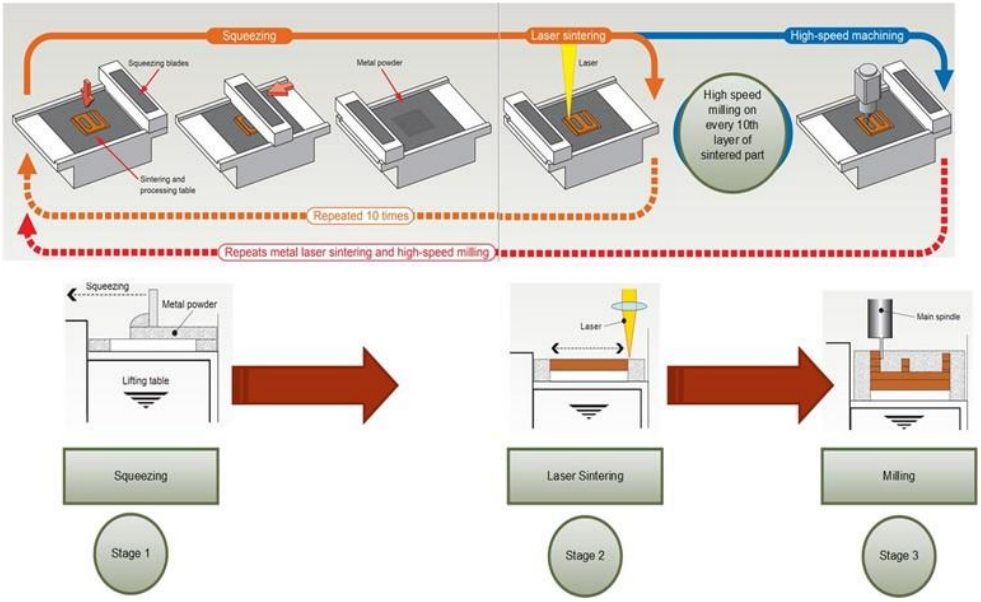


**Figure 2 Direct Metal Laser Sintering Process**

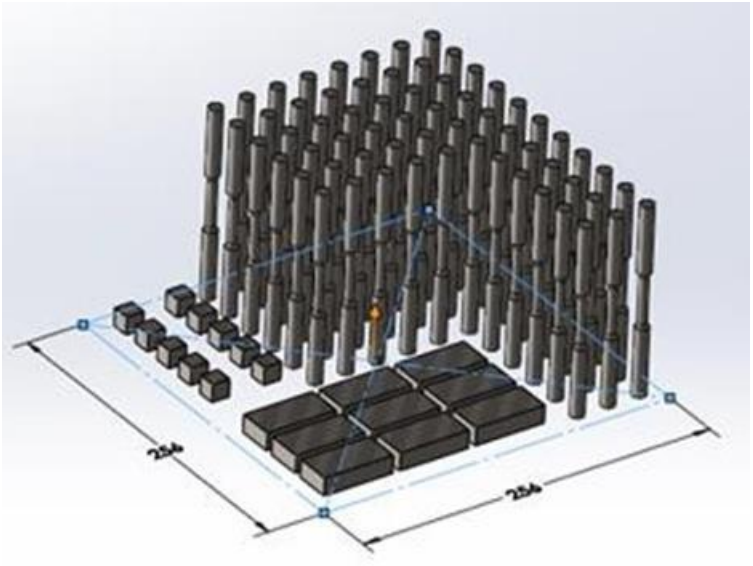


**Figure 3 Built Samples (Along Z-axis)**

## 1.6 Sustainability and Life Cycle Assessment in AM

Earlier, technology to manufacture a product was mainly used based on cost, productivity and technical indicators. However, recently, global warming has become a big concern and industries are forced to reduce the carbon emission.

As highlighted above, AM has provided a substantial superiority over traditional manufacturing operations because of its ability to optimize geometry and produce lightweight parts that encourages the efficient use of material. Moreover, this process eliminates the need of tooling and simplifies manufacturing process by reducing supply chain and transportation cost. Morrow et al. [10] has demonstrated that AM significantly reduces repair cost, energy consumption rate, build cost for customized parts and carbon emission. Presence of these potential benefits are in accord with sustainable process development goals and thus AM is well-suited for sustainability.

Research studies in AM is predominantly focused on sustainability aspects of subtractive machining. Few research studies [11]–[16] that investigate relative performance evaluation of different types of AM with traditional manufacturing process such as injectional molding [14] and subtractive machining [12]. Though these studies provide relative measures of sustainability, these measures are not enough for generalization that AM is sustainable because the energy consumption during AM process largely depends on machine utilization, input parameters type of machine and process used [11], [17]. This study was further substantiated by Faludi et al.[13] who demonstrated that energy efficiency of AM processes is contingent on printing maximum number of parts using minimum number of machines. Given that, few researchers [18], [19] argued metal AM process is energy intensive and involves hidden waste. In fact, further research is needed to understand the breadth of AM sustainability and learn whether AM is in fact energy efficient or environmentally benign. To accomplish a relative environmental performance measures, Bourell et al.[20] calls for the AM sustainability and comprehensive life cycle assessment (LCA).

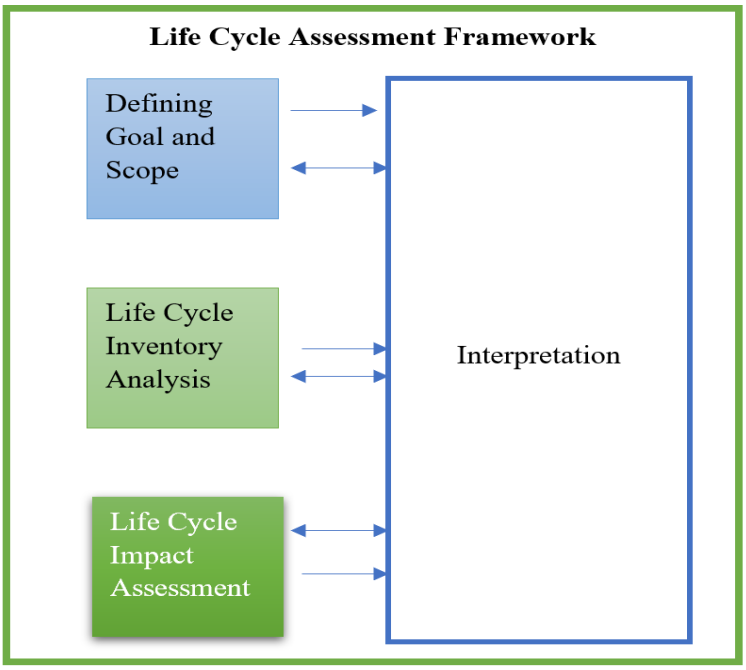


**Figure 4 Stages of Life Cycle Assessment [21]–[23]**

LCA includes the entire life cycle of product and measures material and energy consumption in four stages of product namely extraction, transportation, manufacturing, post manufacturing (product use, reuse, recycling) and disposal to capture the precise view of sustainability. Life Cycle Inventory (LCI) lists, identifies and compiles input resources (material, energy, solvents etc) and output resources (emissions, final product, waste) associated with product life cycle. The overall performance is then evaluated by taking summation of individual energy use, material consumption and emissions in each phase of product life. Use phase of product involves variables such as product type and its use and life cycle inventor Therefore, cradle to gate study has been carried out in this research.

## 1.7 Motivation

DMLS-HM has capabilities of complex geometry generation and near-net shaped geometry and exploits on use of traditional machining to achieve precision and accuracy of manufactured parts. This technology eliminates the need of post processing thus reducing lead time of parts produced. With the growing interest towards AM, expectations have grown from rapid prototyping towards practical applications. Keeping

this in view, in 2009 Roadmap for Additive Manufacturing Report (RAM) by Bourell et al. [20] stresses on the growing need of process and property relationships and developing the sustainable material and sustainable process choices. As hybrid AM is recent phenomenon, very few studies [19], [24], [25] exist that carries out mechanical characterization and energy consumption evaluation. However, these individual studies were restricted to either characterizing mere mechanical properties or finding total energy consumed during the process. Moreover, hybrid process used in these studies were closely relevant to DED process. Among these studies, only Braastad[19] theoretical evaluated the energy consumption and carbon emission. The objective of study by Jackson et al.[25] mainly covered the comparison and evaluation of the energy requirements during hybrid process. Since AM hybrid process is nascent with the inherent additional machining unit integrated, a comprehensive study on mechanical characterization and properties of the printed parts is hardly explored. Also, with the growing concern of sustainable process development, arrival of this hybrid technology calls for need of relative environmental performance with respect to traditional AM and subtractive operations. Therefore, this thesis' objective is to to fill the gaps in the current understanding of hybrid metal AM process and is aimed at the study of both mechanical characterization and eco-impact evaluation of parts produced by LUMEX 25 DMLS-HM.

## 1.8 Scope

For mechanical characterization of the DMLS HM printed parts, Maraging steel 300 (MS 300), a steel alloy powder, has been used. Age hardened and non-aged Maraging steel parts fabricated with DMLS-HM process has been characterized and results were compared to data reported in the literature on conventional DMLS.

For eco-impact evaluation, atomized powder of steel 316L has been assumed as starting material. A physics based energy model considering machine parameters of DMLS HM, EBM machining and conventional machining has been described. This model will serve as basis for eco-impact evaluation. System boundaries are restricted from cradle to gate for life cycle modelling.

## 1.9 Thesis Structure

### 1.9.1 Chapter 2: Literature Review

- Presented overview of published literature related to mechanical characterization
- Description of problem summary and reports the opportunity of research
- Background of eco-impact evaluation and why there is a growing need to opt for sustainable process
- Described some of research studies related to energy consumption modelling and eco-impact evaluation carried out in published literature
- Identified the gap present in DMLS-HM process and objective of this study was presented

### 1.9.2 Chapter 3: Mechanical Characterization of DMLS-HM Manufactured Maraging Steel

- Introduced the experimental procedure, material composition, testing standards and heat treatment methods
- Reported and interpreted results from experimental studies
- Mean effect plots for comparison between DMLS HM and DMLS have been presented
- Deep explanations of these mean effect plots were described

### 1.9.3 Chapter 4: ENERGY CONSUMPTION MODELLING

- Explained in detail on how life cycle assessment would be carried out
- Reported goal and scope of studies and described the functional unit as well as system boundary
- Presented the overview of life cycle inventory (LCI) and listed LCI of steel 316L
- Physical modelling of conventional machining, electron beam melting (EBM), and DMLS HM was presented

### 1.9.4 Chapter 5: Environmental performance evaluation results and discussions

- Energy consumed during these processes were compared on bar graphs.

- A graph between solid to envelope ratio, energy consumption in MJ/Kg (Primary axis and carbon emission in Kg-$CO_2$ (secondary axis) were drawn to understand the energy requirements and comparisons between traditional subtractive and additive processes while fabricating the same geometry

### 1.9.5 Chapter 6: Conclusions and Future Work

- Described the overview of entire thesis studies and presented some of the inferences drawn
- Gave a detailed overview of future work

# CHAPTER 2

# 2 LITERATURE REVIEW

## 2.1 Mechanical Characterization

Amongst the AM processes, powder bed fusion processes such as DMLS or EBM draw more attention due to their ability to make functional parts [26], [27]. DMLS process uses powerful laser energy source to scan and melt a continuous line of powder, one layer at a time. A complex 3-D part can be fabricated by sequential layer creation on top of each other [28]. The process parameters scan speed, layer thickness, powder thickness, hatch size, scan path pattern and laser power will affect the outcome of DMLS process. A part's mechanical properties, surface roughness and geometrical accuracy can all be affected by the settings of these control factors. Over the years, researchers [28]–[31] have reported the effects of these DMLS process parameters on the quality of the part fabricated. Pogson et al. [32] reported that higher scan speeds lead to thinner and longer molten pool while at lower scan speeds more material stay in the molten state. Conventional DMLS parts are fabricated with high surface roughness and density with smaller distance between laser scans as observed by Zhu et al. [33]. Wang et al. [34] reported that among the DMLS process parameters, laser scanning speed and laser power have most significant effect on the density of the fabricated parts. Aging has been known to be effective to improve the strength and hardness of alloy material by formation of intermetallic precipitation. This fact is further supported by studies [31], [35], [36], [37]which have shown that aging of metal alloys produces superior mechanical properties. Azizi et al. [38]carried out microstructural characterization of the as-built and age hardened samples and showed that age hardening effect on maraging steel is similar to material in wrought MS. Moreover, it was demonstrated that virgin powder and re-used powder had the same properties except re-used powder had no flowability. Bhardwaj and Shukla [39] studied the effect of laser scan strategy on surface roughness, texture and tensile strength. They found no significant effect of adopted laser scanning strategy on tensile strength and relative density and these results were comparable to

wrought maraging steel. However, there was an increase in percentage elongation of samples printed in bidirectional strategy because direction of printing was parallel to loading direction. Demir et al. [31] explored the effect of re-melting and preheating on porosity and geometrical error and reported that preheating strategy improves part density and superficial remelting delivers pit free surfaces and induces grain coarsening. It was observed that all remelting strategies resulted into high geometrical errors and poor dimensional accuracies. Casalino et al.[29] reported that specimens with relative high density carry lower porosity and inclusions which in turn result in superior mechanical properties of material. They determined that best mechanical properties can be produced with laser power bigger than 90 W and scan speed lower than 220mm/sec.
Keeping this study in view, samples were produced to get high density. During laser sintering, every layer was re melted keeping same SLM parameter to remove porosity.

### 2.1.1 Problem Summary

DMLS hybrid milling (DMLS-HM) was introduced to improve quality characteristics of fabricated parts and the economy of DMLS process. As described earlier, In DMLS-HM process, an end mill with very high spindle speed and high feeding rate is incorporated with the laser sintering to attain high-precision machined surfaces. The sintering and milling of the part are repeated to build from bottom to top layers of a complex part shape and will produce much better surface finish. Some industrial applications such as mold runners require surface roughness to be as low as 0.3µm to avoid any sudden or early failure from surface-initiated cracks [27]. Wang et al. [34] reported that low surface quality results in poor accuracy and negatively impacts strength, wear and corrosion resistance. Compared to conventional DMLS, there is limited knowledge on the mechanical properties of parts fabricated with DMSL-HM process.

### 2.1.2 What must be done

This research uses experimental and analytical approach to evaluate as-sintered and heat-treated Maraging steel 300 (MS 300) parts fabricated with DMLS-HM process and quality characteristics will be compared to data reported in the literature for conventional DMLS.

## 2.2 Eco-Impact Evaluation

Mechanical machines require electrical energy to drive its auxiliary units (motor, spindle or shaft). The more efficient a mechanical operation is, lesser energy is consumed. With the growing concern over carbon emission, governments are forcing industries to reduce carbon emission. It is in the interest of industrial organization to make an effort towards improving the energy efficiency. Therefore, a comprehensive research studies analyzing energy consumption will help understanding how electrical energy is distributed in AM machine. This section provides the overview of studies that has been done on energy requirements and environmental impact over the years.

### 2.2.1 Conventional Machining

Conventional machining (CM) operation refers to subtractive operations used to remove the material from workpiece. Modern CM's function includes lubrication, tool changing, work handling operation, and tool break detection. Power requirements in machine tool can be calculated analytically using either cutting force or thermal equilibrium. To achieve the desired surface geometry and especially surface finish, subtractive operations are generally necessary. However, this process will come at the expense of significant processing time and input energy resources. Therefore, for thorough understanding of energy requirements in CM, one needs to understand important aspects of energy requirements and how power demand is spread among machine components. Cooperative Effort on Process Emission in Manufacturing (CO2PE) [40] proposed a methodology to standardize the energy collection data so that collected energy values can be presented around the world. This approach classified energy requirements into two operational states: basic state and cutting state. In basic state, electrical energy is needed to turn on machine components and making sure that it is ready for machine operation. Cutting state involves the use of tool to remove material from workpiece. Balogun and Mativenga [41] argues that CO2PE does not clarify transitional stage between basic state and cutting state which in this study will be called 'ready state'. They argue that ready state needs to be introduced to capture energy requirements once the machine is started. Dahmus and Gutowski [42] found out that around 14% of electrical energy is consumed in actual material removal operations and around 86% of energy is consumed during idle

and basic operations. Their findings have been further substantiated by Balogun and Mativenga [41] and Diaz et al. [43].He et al. [44] estimated the energy consumption by correlating the numerical control (NC) codes and energy consuming components. They projected the feed time, cutting time, pump running time from NC codes and used the specific cutting force to estimate energy consumption. Balogun and Mativenga [41] describes the limitation of this model and argues that specific energy is relatively more holistic for energy estimation as compared to specific cutting force. Since, specific cutting force does not consider energy consumption of auxiliary units such as fans, computer, chiller, tool changes etc. Also, methodology of cutting force is not applicable for all machines.

Notable contribution in specific energy context in subtractive systems was made by Gutowski et al. [42] by introducing a novel mathematical model for the first time for energy requirement in milling. This work was further improved on by Mori et al. [45] and Diaz et al. Gutowski et al.[42] and Diaz et al[43] acknowledges that tool engages and disengages with the workpiece during machining operation. And not all cutting time is consumed in removal process. This gave the hint to Balogun and Mativenga [41] who coined the term ‘air cutting time’ of toolpath to understand the impact of energy consumed when tool disengages with workpiece while cutting. Specific energy based mathematical models developed by these researchers [41]–[43], [45] are fundamentally important to understand the energy consumptions in machine toolpath and auxiliary components and will help evaluating energy efficiency and resultantly will help to reduce machine cost and energy footprints. Subtractive machining is inherently more wasteful which renders CM less attractive choice for sustainable planning and development. Munoz et al.[46] provided an analytic approach to examine environmental impacts. Ingarao et al.[47] compared the environmental performance of hot extrusion and machining process. LCA based approach was implemented on a simple aluminum part, manufacturable from both manufacturing techniques and energy flows occurring during extraction, production and end of life phase of simple aluminum geometry were recorded. They found out that optimal and sustainable process selection largely depends on batch size. It was demonstrated that for low production volumes, machining approach is more feasible.

### 2.2.2 Additive Manufacturing

AM offers an excellent opportunity of increasing resource efficiency as it produces little to no waste, thus providing an alternative sustainable operation unlike subtractive machining which is relatively more wasteful. However, despite giving such positive hope, AM has not been explored much from sustainability point of view [48]. This is because AM is a nascent technology having relatively lower research studies on sustainability. Majority of studies in metal AM are confined to modelling energy requirements. Baumer et al. [49] carried out the comparative assessment of selective laser melting (SLM) and ARCAM A1 Electron Beam Melting (EBM) on a 'spider shaped standardized geometry' . They found out that EBM consumes relatively less energy for both single build part experiment and full build part experiment. Lower energy consumption in EBM was partly credited to its high build rate (high material thickness). In another study, Baumer et al. [50] investigated the correlation of sample geometry with energy consumption in Electron Beam Melting (EBM). They found weak correlation between complexity of geometry and energy consumed by EBM. It was reported that smart tools such as topology optimization provides optimal geometries and increased cost has no bearing on cost of finished parts. Furthermore, they found out that a single part consumes relatively more energy than same full-build parts printed simultaneously. Morrow et al.[10] quantified energy consumption and environmental impact associated with processing of mold and tooling when manufactured by AM variant called direct metal deposition (DMD) and CNC milling operations. Their research concluded that samples with low solid-cavity ratio in DMD consumed less energy than CNC milling and sample with high solid-cavity ratio is more economical when manufactured through CNC milling. Mognol et al.[51] found out that part orientation influences the energy consumption. They proposed that manufacturing time influences energy consumption and to reduce manufacturing time, Z-height of geometry should be reduced. Peng and Sun [52] developed an analytical model for quantification of energy consumption in fused deposition of thermoplastics.

Bourhis et al. [16] proposed a new analytic methodology to accurately evaluate the environmental impact using its CAD model in direct metal laser sintering. Their research focused not only on direct energy requirements but also fluid and material consumption

associated with operation. Faludi et al.[13] compared environmental impacts of additive and subtractive machining in plastic production. This study was first of its kind which comprehensively recorded not only waste or $CO_2$ emission but also other impact categories such as acidification, eutrophication, human toxicity, ecotoxicity.

### 2.2.3 Additive-Subtractive (Hybrid) Machining

Studies on energy modelling of additive hybrid subtractive manufacturing systems are limited. Jackson et al.,[25] were first to develop energy model that accounted for energy consumption during metal production, deposition and machining phases in additive-subtractive manufacturing hybrid system. Their work compared the energy consumed by powder-based additive-subtractive manufacturing systems with wire-based additive manufacturing and concluded that processing energy in both processes are the same.

### 2.2.4 Problem Summary

Electrical energy produced by renewable sources have little to no impact on environment. United States Environmental Protection Agency (EPA) reports that predominant source of carbon footprints in USA is from burning non-renewable fossil fuels used to generate electricity. Also. industrial sector is responsible for 22% of electricity consumption and around 24% of green- house gas emission [53]. Jeswiet and Kara [54] demonstrated a direct link between carbon emission and electrical energy requirement and found out that with the increase in demand of product and services, the energy demand is growing proportionately, which is resulting into proliferation of carbon footprint.

The resulting carbon emission is growing concern in the world and leaders around the world are making efforts to curb emission by putting carbon tax on industries. This has put stakeholders of industry under pressure to mitigate footprints. Therefore, it is imperative from industrial perspective to manufacture goods that produce low carbon footprint per unit to make it acceptable across the world. So, it is high time to research the basic physics of energy consumption in machine components and develop accurate models which analytically evaluate energy requirements in manufacturing operation. Thus, helping researchers and engineers in making informed decision about a sustainable process.

Studies from literature review suggest that majority of studies discuss about energy consumption during operation in metal AM. Very few studies [11], [16], [19], [48] exists that evaluates and analyses the sustainable perspective of metal AM. It is important to note that DMLS HM, a hybrid technology, is novel in its entirety. This technology eliminates the need of post processing thus reducing lead time of parts produced. Given these benefits, researchers [25],[55] claim that hybrid manufacturing (HM) may offer greater opportunity for sustainable manufacturing and use of HM could reduce the environmental burden. However, it would be premature to call HM sustainable without a comprehensive life cycle assessment. From literature survey, it was found that scope of the majority of studies [56],[11], [14] focused their work on AM and were limited to measuring operational energy consumption during process. Very few studies [57], [15] characterized environmental impacts of AM. Since DMLS-HM is new technology, study on quantitative analysis of its energy consumption has been largely unknown.

### 2.2.5 What must be done

There need to be a theoretical energy framework by which researchers can estimate energy consumed during the process. This research will close some of the gap in knowledge by using analytical model approach to compare energy consumption and eco impact of DMLS-HM with two others competitively used manufacturing processes: conventional machining (CM) and electron beam manufacturing (EBM).

# CHAPTER 3

# 3 MECHANICAL CHARACTERIZATION OF DMLS-HM MANUFACTURED MARAGING STEEL[1]

## 3.1 Introduction

Atomized powder of Maraging steel 300 was used as a raw material. Mechanical properties of samples printed from DMLS HM has been compared with conventional DMLS.

## 3.2 Experimental Procedure

ASTM standard dimensions were followed during preparation of test samples. Destructive tests such as hardness, tensile testing, toughness were carried out for both as-built and heat treated samples to characterize mechanical properties and identify the level of variability. All the test samples were printed vertically (along Z-axis) with the layer oriented perpendicular to the load direction

### 3.2.1 Material

Maraging is classified as a low-carbon, ultra-high strength steel. Its name is derived from a combination of '*mar*tensite' – a very high strength phase of steel and '*aging*'. Maraging steel 300 (MS 300) can be age-hardened to increase its strength and hardness properties by significant amounts. The MS 300 alloy powder used in this study was produced by gas atomization with composition given in Table 2.

**Table 2 Maraging Steel Powder, Percent Composition by Mass [58] (Renishaw)**

| Element | Fe | Ni | Co | Mo | Ti | Al | Cr | Mn, Si | P | S |
|---|---|---|---|---|---|---|---|---|---|---|
| Wt. % | Bal. | 17-19 | 7-10 | 4.5 – 5.2 | 0.3-1.2 | 0.05-0.15 | ≤0.5 | ≤0.10 | ≤0.03 | ≤0.01 |

[1] Under Review in Journal of Manufacturing

### 3.2.2 Tensile Test Specimen

The specimen for the tensile tests (Figure 5) is designed to the standard geometry listed in ASTM Standard E8 [59]. The critical geometry of this specimen is the necked down region. This necked down region ensures the specimen breaks in a predictable manner. Tension tests were performed at room temperature on 28 Maraging steel specimens using MTS Landmark tensile testing machine with 55 Kips load cell. Engineering stress strain curve was used to evaluate the mechanical properties: yield strength, ultimate tensile strength, modulus of elasticity, modulus of resilience, and ultimate tensile strain

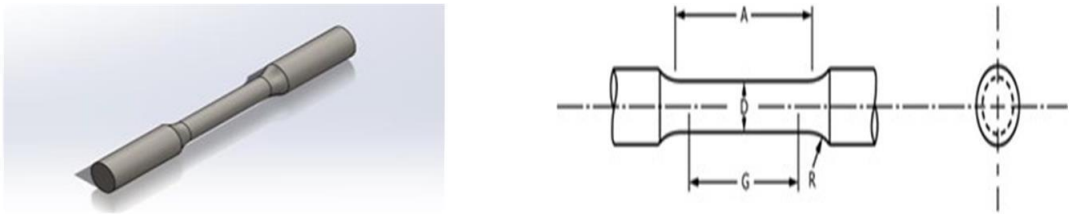


**Figure 5 Tensile Test Specimen (ASTM E8)**

**Table 3 Standard Dimensions for Tensile Specimens**

| Feature | Dimension |
|---|---|
| G - Gauge Length (mm) | 25.4 ± 0.127 |
| D – Diameter (mm) | 6.35 ± 0.127 |
| R - Radius of Fillet (mm) | 4.8 |

### 3.2.3 Hardness Test Specimens

Test specimen (figure 6) was designed in accordance with ASTM standard E18 [60]. Two different machines: Wilson Rockwell and Fowler Rockwell hardness tester were used to conduct hardness tests using Rockwell C scale with 120º sphero-conical diamond head.

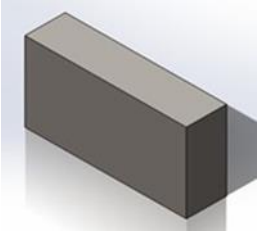

**Figure 6 Hardness Testing Specimen**

**Table 4 Dimension of specimens for hardness and density**

| | Hardness | Density |
|---|---|---|
| Length (mm) | 50.8 | 12.7 |
| Width (mm) | 25.4 | 12.7 |
| Thickness (mm) | 12.7 | 12.7 |

### 3.2.4 Charpy Impact Test Specimen

Charpy impact test was conducted to measure toughness of the samples in accordance with ASTM E 23[61]. The size of specimen was 55x10x10 mm with notch defined by standard. Tinius Olsen Charpy Impact tester was used for toughness testing at room temperature.

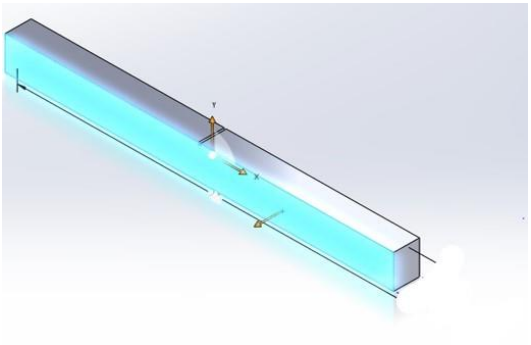

**Figure 7 Charpy impact test specimen**

### 3.2.5 Surface Roughness and Density

A portable Mitutoyo Surftest SJ-210 was used to measure the surface roughness of the parts made with DMLS-HM process. The Mitutoyo Surftest SJ-210 provided numerous measurement statistics including the graph of the surface roughness.

Analytical balance of high precision was used to calculate weight in air and demineralized water. Taking density of water 0.9982 g/cm$^3$ at 20ºC, the average relative density was 99.5% for age hardened components.

## 3.3 Results and Discussion

## 3.4 Mechanical Properties Before Heat Treatment

### 3.4.1 Tensile Properties

Table 5 shows the comparison of tensile properties of Maraging steel produced by DMLS-HM and conventional DMLS obtained from literature. Figure 8 shows the stress strain curves of the maraging steel samples made with LUMEX DMLS-HM. The tensile properties of the 28 samples show minimal variation between each other.

**Table 5 Comparative Tensile Properties for DMLS-HM vs DMLS of Maraging Steel**

| Mechanical Property | DMLS-HM | DMLS |
|---|---|---|
| Yield Strength (MPa) | 1111.5 | 915 [36] |
| | 1101.5 | 780-925 [30] |
| | 1121.5 | 720-900 [37] |
| Tensile Strength (MPa) | 1205.5 | 1290 [62] |
| | 1215.5 | 1178 [63] |
| | 1195.5 | 1165 [30] |

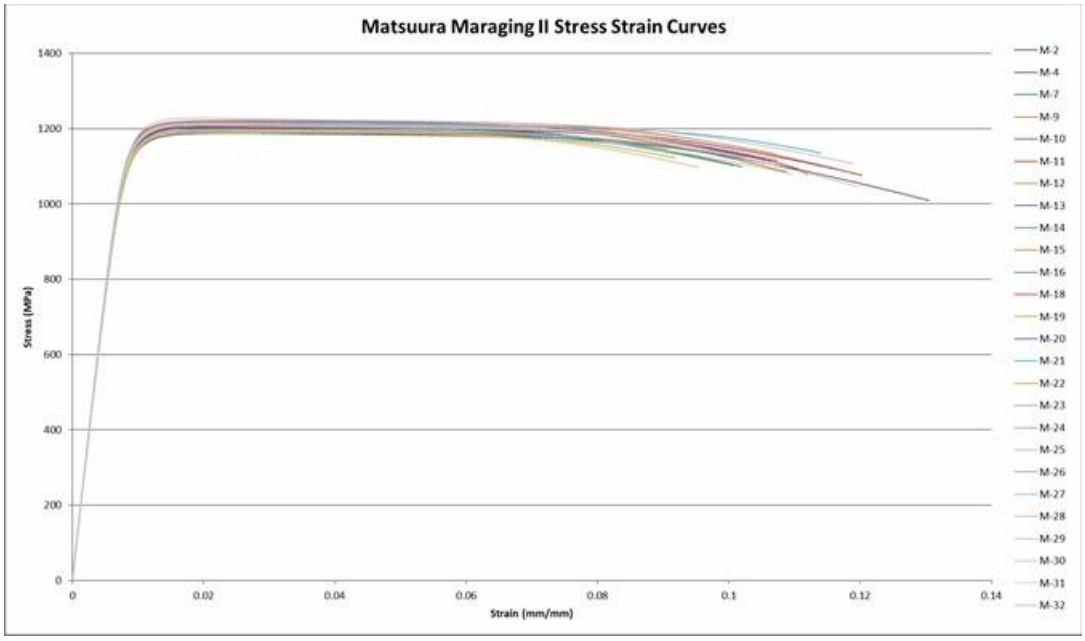


**Figure 8 Stress-Strain Curve of Maraging Steel Produced from DMLS-HM**

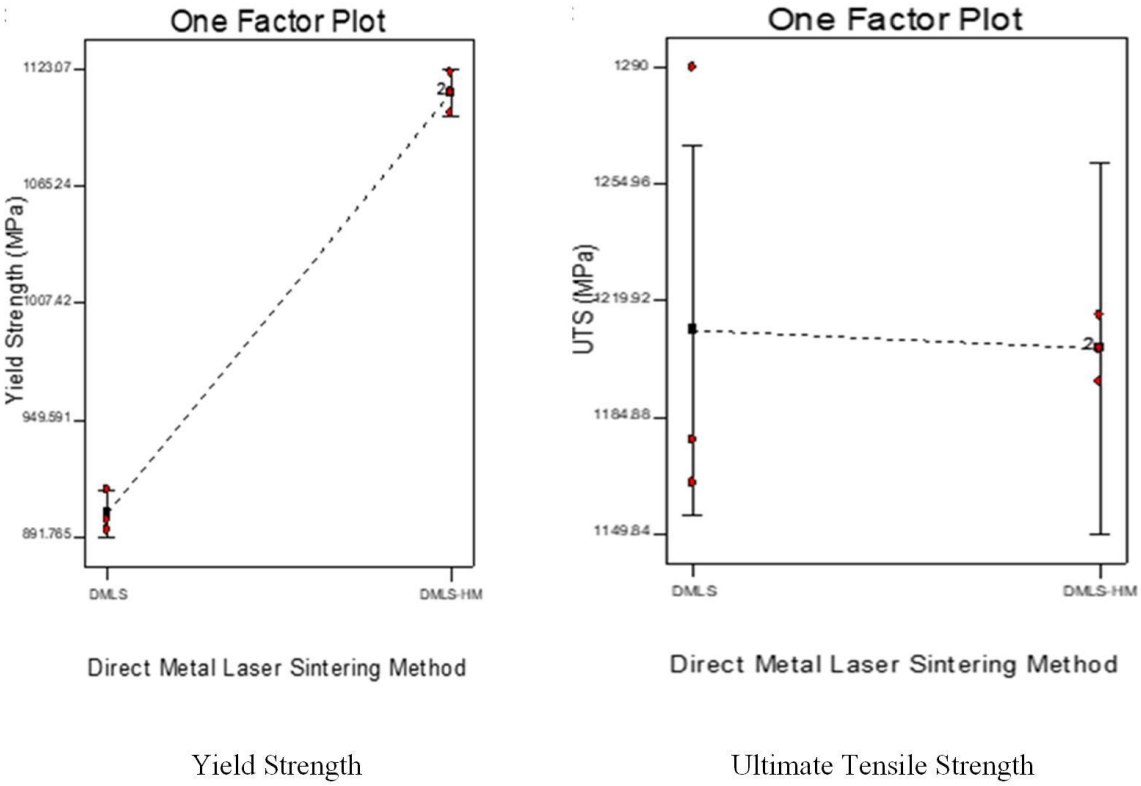


Yield Strength Ultimate Tensile Strength

**Figure 9 Mean Effect of DMLS-HM on Tensile Properties of Non-Aged Maraging Steel**

DMLS-HM process has significant effect on the yield strength of non-aged Maraging steel. There is very little chance that the average change due to use of DMLS-HM is caused by noise. However, the ultimate tensile strength is not significantly affected by use of DMLS-HM process. The variation within the sample of data obtained from different authors is too large that the model is not significant relative to noise as shown in Figure 9.

### 3.4.2 Toughness Property

Table 6 shows the toughness properties of Maraging steel produced by DMLS-HM and obtained from Charpy Impact test versus conventional DMLS reported in literature. ANOVA was conducted on the data and mean effect plot of the DMLS techniques is shown in Figure 10. DMLS-HM process has significant effect on the toughness of non-aged Maraging steel. There is an average of 56% increase in toughness of non-aged Maraging steel by using DMLS-HM to form them.

**Table 6 Average Toughness of DMLS vs DMLS-HM**

| DMLS-HM (J) | DMLS (J) |
|---|---|
| 94.71 | 42 [63] |
| 95.64 | 45 [64] |
| 101.69 | 40 [62] |

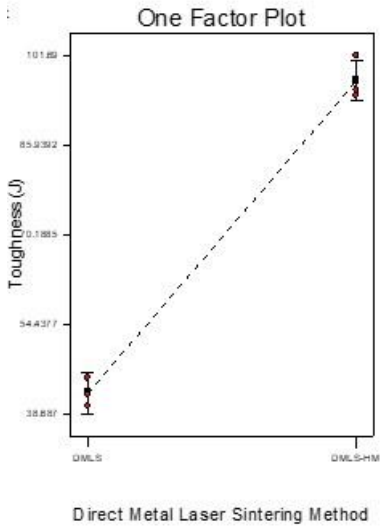


**Figure 10 Mean Effect of DMLS-HM on Toughness Properties of Non-Aged Maraging Steel**

### 3.4.3 Surface Roughness

Surface roughness of finished Maraging steel parts formed with DMLS-HM and DMLS are shown in Table 7. The data indicates that most DMLS surface roughness is in the range of 4-22µm. ANOVA was conducted on the data and mean effect plot of the DMLS techniques is shown in Figure 11. The effect of DMLS-HM shows statistical significance and resulted in average reduction in surface roughness of 42%. Results show that commercial DMLS machines would require post processing operations like shot peening or polishing; while the DMLS-HM machines would not need any of those post surface operations. The anticipated benefit is shortened lead time and reduction in manufacturing cost. Figure 13 shows the non-polished fresh morphologies and roughness of DMLS-HM fabricated Maraging steel specimens. The paralleled laser tracks are shown (figure 13 right side) and strips indicate overlap zone of two laser irradiation tracks. There are many unmelted powder particles absorbed on the vertical surface of the DMLS therefore keeping the roughness around 4.16 micrometer.

**Table 7 Surface Roughness of DMLS-HM and DMLS**

| DMLS-HM (µm) | DMLS (µm) |
|---|---|
| 0.2454 | 15-22 [29] |
| 0.1626 | 4.16 – 4.79 [30] |
| 0.2057 | 4.01 – 6.01 [31] |

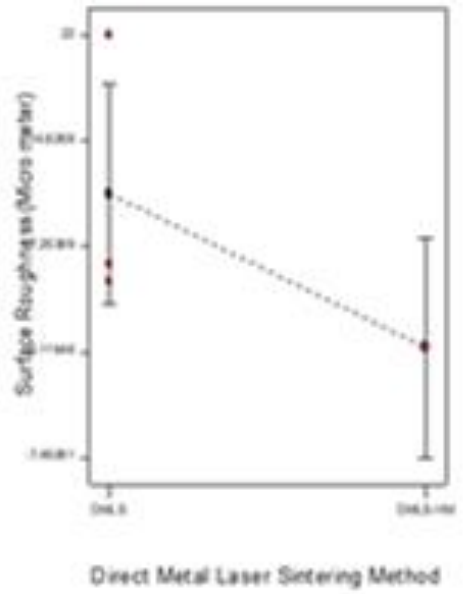


**Figure 11 Mean Effect of DMLS-HM on Surface Roughness of Non-Aged Maraging Steel**

### 3.4.4 Hardness

The hardness property of the Maraging steel parts formed with DMLS-HM and the DMLS data obtained from literature are shown in Table 8. ANOVA was used to analyze it and mean effect plot of the DMLS techniques is shown in Figure 12. The effect of DMLS-HM does not have statistical significance with a lot of variability in the reported hardness data of DMLS parts.

**Table 8 Hardness of DMLS-HM and DMLS**

| DMLS HM | DMLS |
|---|---|
| Hardness (HRC) | Hardness (HRC) |
| 37 | 40 [62] |
| 36.1 | 35 [30] |
| 36 | 41 [63] |

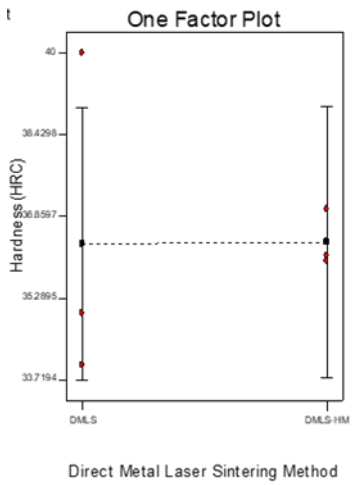


**Figure 12 Mean Effect of DMLS-HM on Hardness of Non-Aged Maraging Steel 300**

### 3.4.5 Macro and Microstructural Evaluation

Characterization and evaluation of surface roughness of manufactured parts are of great importance because it affects the modeling accuracy of parts made by direct metal laser sintering process. Figure 13 shows non-polished fresh morphologies and roughness of MS 300 samples made with DMLS-HM and DMLS. The paralleled laser tracks are overlap of two laser irradiation tracks is observed on both processes. For DMLS in Fig. 13 (right side), many umelted powder particles adsorbed on the vertical surface because the fabrication process is embedded in the powder bed and the powders are easily attached to the cross-section of uncooled sintered layers by Tan, Chaolin, et al. [30]. This surface condition is not observed with samples made with DMLS-HM as a result of hybrid high speed milling process that takes place during the fabrication as shown in Figure 13 (left side). Figure 14 shows the micro structural graphs of tensile fracture of non-age hardened MS 300 made by DMLS-HM versus DMLS from literature. The samples experience large plastic deformation with formation of significant number of micro cavities arising at the precipitates or imperfections sites in the material. These micro cavities will create stress intensities resulting in more micro-cavities. The originated micro-cavities will conjoin and the growing tears that will cause the material's fracture in ductile mode. A ductile fracture is always trans-granular in nature as shown in Figure 14. The distinctive difference between DMLS-HM and DMLS is the shallower

dimples in the DMLS which lead to relatively higher plastic deformation. The resultant higher tensile properties (yield strength, tensile strength, and hardness) of non age-hardened MS 300 made by DMLS-HM are more attractive for its applications such as tools and mechanical components.

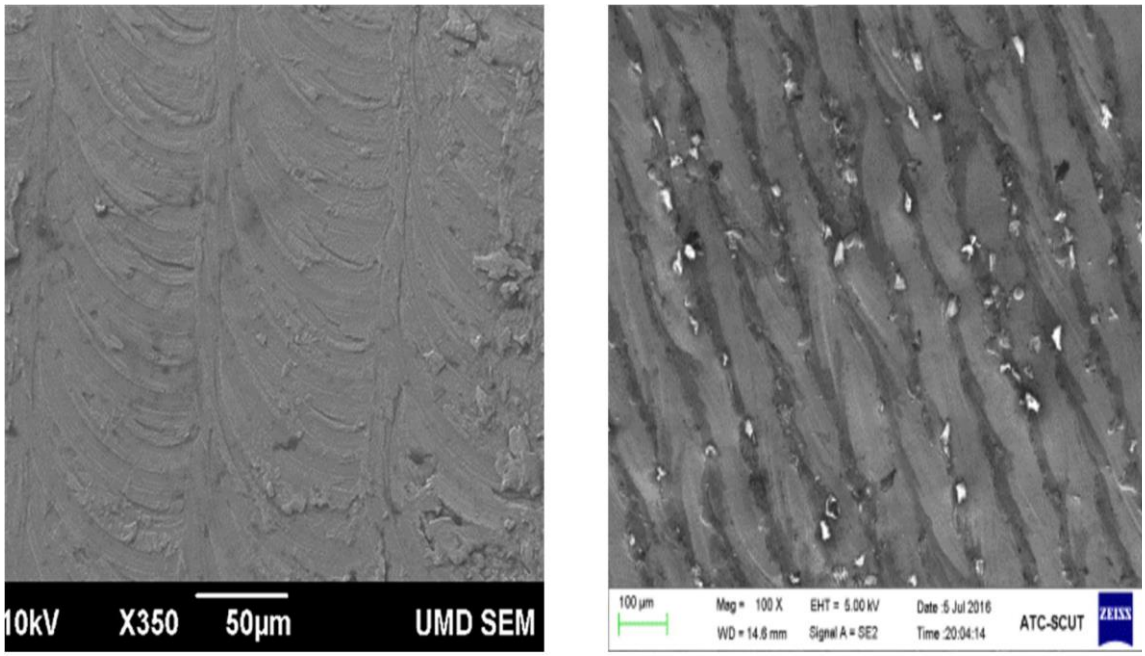


DMLS-HM with about 0.20 µm

DMLS with about 4.16 µm

**Figure 13 Top horizontal Surface morphology and roughness**

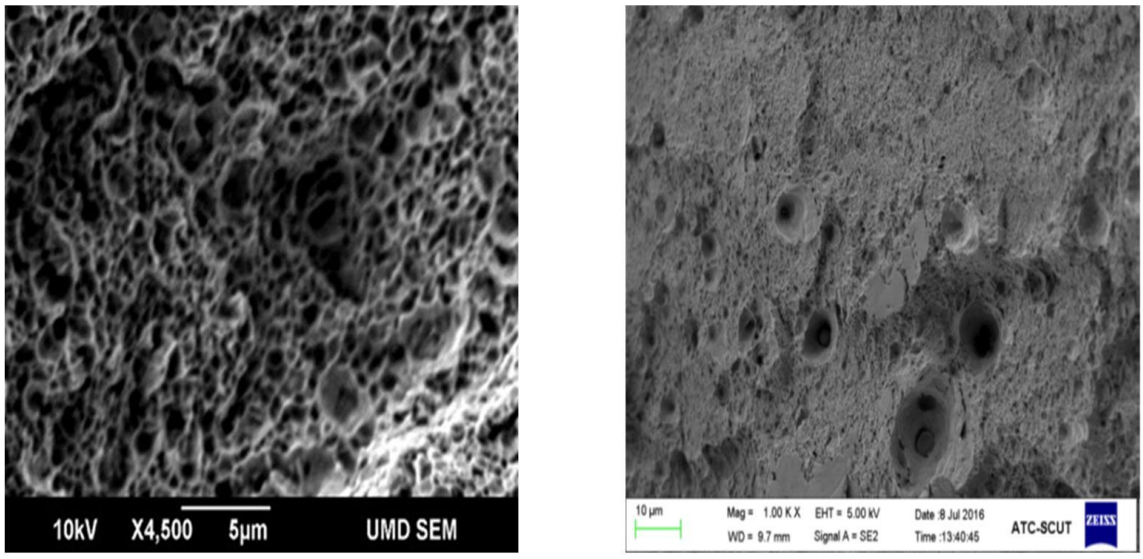


DMLS-HM DMLS

**Figure 14 Tensile Fracture Surface morphology of Non-Age Hardened MS 300**

## 3.5 Mechanical Properties Post Solution Heat Treatment

Maraging steel possesses high strength as well toughness and often used in high duty applications. Superior mechanical properties of MS 300 are attained by heat treatment through solution treatment and aging treatment. During age hardening, intermetallic precipitates such as Ni3 (Mo, Ti) and Fe2Mo phases are formed, which will disturb the movement of dislocations. Kempen et al. [62] reported that optimal age hardening conditions for superior mechanical properties is aging at 480º C for 5 hours for MS-300. Total of three samples of each test specimens of the DMLS-HM parts were solution heat treated at 815 º for one hour, followed by aging in an oven at 480º C for 5 hours. After heat treatment was completed, their tensile, toughness and hardness properties were evaluated. The heat treatment conditions were kept consistent to maintain comparative evaluation of the samples.

### 3.5.1 Post Heat Treatment Tensile Properties

Post heat treatment tensile properties property of the DMLS-HM samples have shown significant improvement as seen in Table 8. The comparative post heat treatment tensile properties of DMLS show similar data with slight increase. The mean effect of the

process does not have statistical significance. ANOVA shows that there is no difference in the tensile properties after the samples are heat treated as illustrated by Figure 15.

**Table 9 Post Heat Treatment Tensile Properties for DMLS-HM vs DMLS of Maraging Steel 300**

| Mechanical Property | DMLS-HM | DMLS |
|---|---|---|
| Yield Strength (MPa) | 1835 | 1957 [36] |
| | 1827 | 1833.3 [37] |
| | 1842 | 1793 [30] |
| Tensile Strength (MPa) | 1902 | 2017 [36] |
| | 1895 | 2088 [37] |
| | 1909 | 2216 [62] |

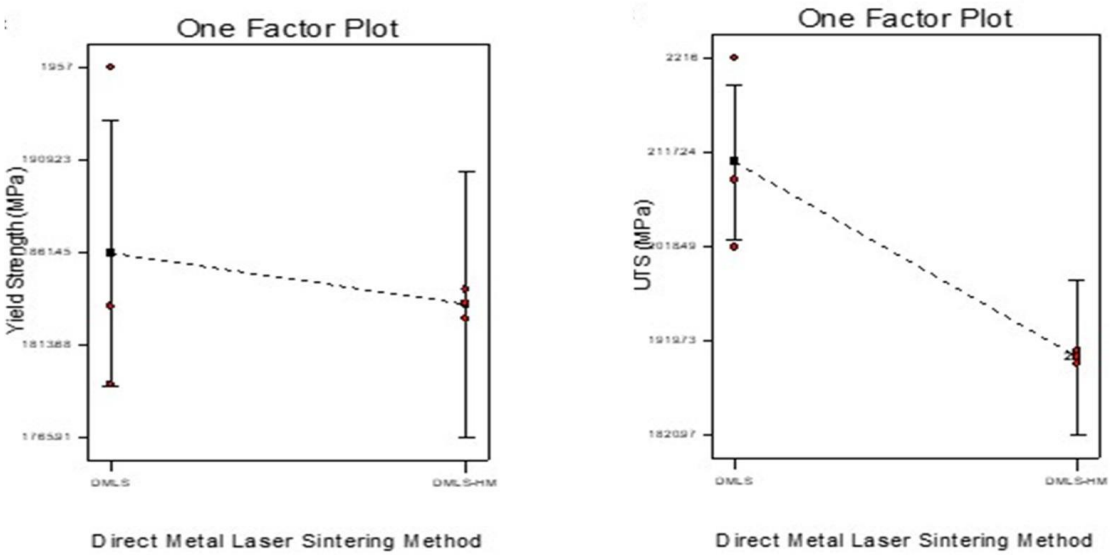


**Figure 15 Mean Effect of DMLS-HM on Tensile Properties of Heat Treated Maraging Steel**

### 3.5.2 Post Heat Treatment Toughness and Hardness Properties

Heat treatment of the Maraging steel samples was conducted by solution heat treatment and aging treatment. The Maraging steel samples formed by DMLS-HM decreased its toughness property by 69% from 92J to 28J as shown on Table 10. This significant decrease in toughness is attributed to intermetallic precipitation of compound because of aging[63]. When toughness of DMLS-HM is compared to DMLS parts after heat treatment, the DMLS-HM samples maintained toughness property that is four times higher than the DMLS samples as show in Figure 16

**Table 10 Post Heat Treatment Toughness and Hardness Properties for DMLS-HM vs DMLS of MS 300**

| Mechanical Property | DMLS-HM | DMLS |
|---|---|---|
| Toughness (J) | 28.2 | 7 [62] |
| | 28.3 | 8[63] |
| | 28.4 | 10 [64] |
| Hardness (HRC) | 54.4 | 58 [62] |
| | 54.3 | 56.2 [24] |
| | 54.22 | 52 [30] |

The hardness properties of the DMLS-HM and DMLS samples presents similar values as is shown in Table 10. There was about 33% increase in hardness after aging for samples made by both techniques. This improvement in hardness is because of precipitation hardening. Ni, Mo and Fe dissolved in matrix filter out in from of Nickel rich compounds like $Ni_3Mo$, $Ni_3Ti$, which generate precipitation hardening [62]. This second phase precipitates significantly resist movement of dislocations and substantially improves hardness.

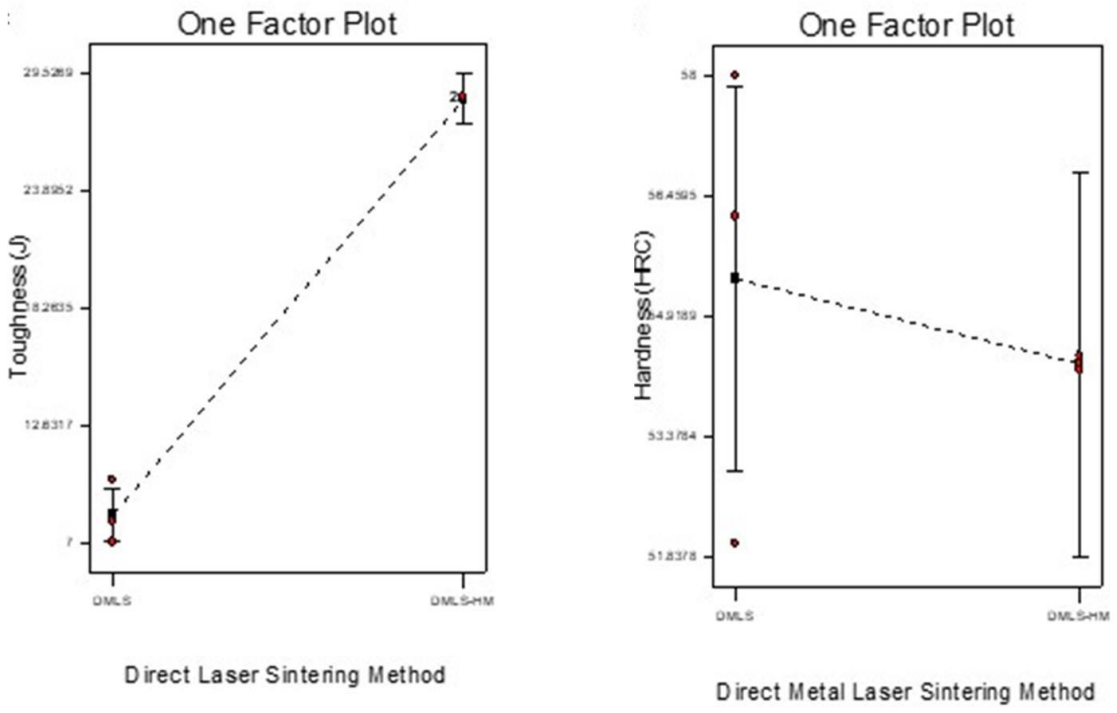


**Figure 16 Mean Effect of DMLS-HM on Toughness and Hardness Properties of Heat Treated MS 300**

## 3.6 Conclusions

The goal is to benchmark quality characteristics of samples made with direct metal laser sintering hybrid milling process in contrast to those made with conventional direct metal laser sintering data reported in literature. The influence of process parameters in the comparative analysis is minimized by using authors' data that were obtained with similar process parameter levels. Comprehensive tests and evaluations of mechanical properties and surface conditions of both as-sintered and age hardened Maraging Steel 300 samples made with LUMEX direct metal laser sintering hybrid milling (DMLS-HM) were accomplished.

DMLS-HM process had significant effect on the toughness of as-sintered MS 300 samples. There was an average of 125% increase in toughness of as-sintered MS 300 made with DMLS-HM compared to DMLS parts reported in the Literature.

As anticipated, DMLS-HM showed statistically significant effect on surface roughness of fabricated MS-300 samples resulting to average reduction in surface roughness of 42%

compared to parts made with DMLS. The level of surface finish obtained with DMLS-HM will allow use of this process to make parts without the need of post processing operations like shot peening or polishing. The large impact of achieving machined surface finish with DMLS-HM can be seen in manufacture of components with inaccessible features to conduct finish operations such as mold inlets.

In addition, the DMLS-HM process showed significant effect on the tensile yield strength of MS-300 sample compared to conventional DMLS. There was 22% average increase in yield strength of parts made while the effect on ultimate tensile strength did not show statistical significance.

The overall mechanical properties of as-sintered DMLS-HM components increased significantly after heat treatment except their toughness property that experienced significant decrease as anticipated. The macro-structural evaluations using scanning electron microscope showed that surface morphology of DMLS-HM had the surface finish of a machined surface with very low roughness number in the range of 0.2 µm. The conventional as-sintered DMLS process will have much rougher surface condition in the range of 4 to 22 µm that will require post processing to achieve desired surface finish. However, post processing may not be possible for some applications such as manufacture of molds with interior channels. The micro-structural evaluations showed that DMLS-HM samples had distinctive deeper dimples in their fracture surface that lead to resultant higher mechanical properties (yield strength, tensile strength, toughness, and hardness) at as-sintered state. This makes the process more attractive than conventional DMLS for applications such as molds and tools manufacture.

# CHAPTER 4

# 4 ENERGY CONSUMPTION MODELLING[23]

## 4.1 Introduction

It starts with the overview of methodology used followed by goal and scope of life cycle assessment boundary. Life cycle inventory keeping in view the system boundaries has been listed. To calculated energy consumption, origins of analytic based model for EBM and conventional subtractive machining has been described.

## 4.2 Methodology

Figure 17 shows typical four stages of a product life cycle beginning from extraction, material production, product manufacture and product use. The stainless steel 316L (SS 316L) grade is the second most common austenitic stainless steel with primary alloying constituents after iron, chromium (16–18%), nickel (10–12%) and molybdenum (2–3%). The addition of molybdenum provides MS with greater corrosion resistance than stainless steel 304. Some of its major applications include in chemical and petrochemical industry, potable water and wastewater treatment, marine applications and architectural applications near the seashore or in urban areas. Steel production starts with material extraction from natural ores and during production, recycle percentage of scrap stainless steel in current supply of raw material is in the range of 35-40%[23]. Embodied energy of SS 316L is the energy consumed by all the processes associated with the production of SS 316L, from the mining and processing of natural resources to manufacturing, transport and delivery. The primary material production energy is usually energy intensive process and energy consumption is higher than material produced from scrap steel. For example,

[2] Under Review in Journal of Heliyon
[3] Poster paper accepted for NAMRC 47 conference proceedings at Penn State University

stainless steel's embodied energy from recycling is around 22-25 MJ/kg and embodied energy during primary production of material is 77-85 MJ/kg.

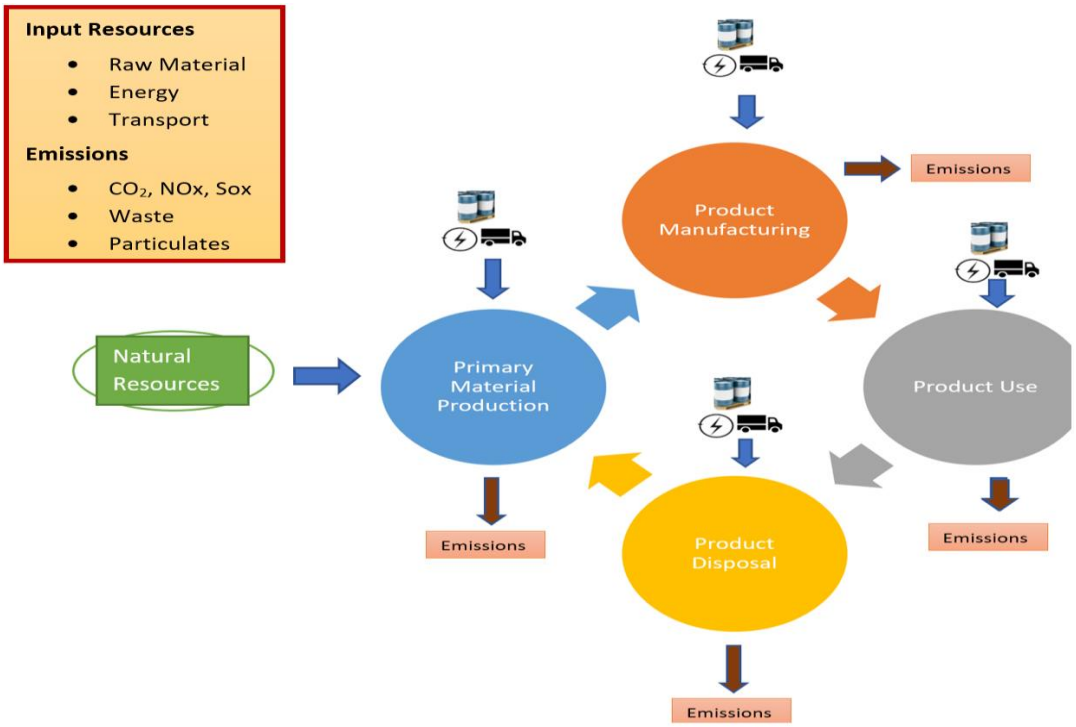


**Figure 17 The material life cycle showing consumption of energy and materials and emission of waste heat, solid, liquid, and gaseous emissions (Modified) [23]**

## 4.3 Goal and Scope

The goal is to develop an analytical model of energy consumption for DMLS-HM process and use this model to evaluate total energy consumed during processing of stainless steel 316L part. Further, the total energy consumed, and environmental impact of DMLS-HM are compared with conventional milling and electron beam melting (EBM) processes for manufacturing of the same part geometry.

## 4.4 Functional Unit

The functional unit is used to provide a reference where the life cycle analysis inputs and outputs are standardized. The functional unit established for this study is one unit of Stainless Steel 316L produced.

## 4.5 System Boundary

The system boundary is used to define which processes from the life cycle assessment analysis will be included or excluded. The life cycle analysis will track the inputs and outputs from each of the unit processes of DMLS-HM, conventional milling and EBM from resource extraction and processing to transportation and to emission control measures. In this study, the system boundary includes all the stages starting with material extraction from natural resources, to material processing and part manufacturing. The energy consumption during the product's usage and disposal is not considered.

## 4.6 Energy Model & Life Cycle Inventory (LCI)

The assessments and comparisons are based on the total energy consumption and environmental impact assessment of three samples of 316L steel with three different geometries, each manufactured through three distinct processes namely: conventional milling, EBM and DMLS-HM. The total energy consumed from cradle to gate by each process was determined. The data on energy consumed during primary metal production as well as material shaping/forming processes such as extrusion and rolling was collected from Gabi database and other published literature. Few authors [22],[65] have described the discrepancies in the available data knowledge. Keeping this in mind, rigorous effort has been made to assure good representation of the data by taking average of collected energy consumption values. Moreover, the energy values for machine parameters and process environment were kept consistent. The energy consumption during each unique process was estimated analytically, using standard machine parameters as suggested by machine manuals for producing the final parts. The solid-envelope ratio as employed by Watson and Taminger [66] was used as a common framework to compare energy efficiencies of these processes. The solid-envelope ratio is the ratio of volume of solid material and the bounding volumetric envelope of part denoted with α in this paper. It is used to estimate total energy required by the three different processes to manufacture the parts to their final geometries. Each geometry considered has a unique value of α that will capture the energy requirement in the process used to make it. Table 11 shows the life cycle inventory of stainless steel 316L and how they were obtained for this work.

**Table 11 Life Cycle Inventory of Stainless Steel 316L**

| Energy Consuming Processes | Energy (MJ/kg) | | Reference |
|---|---|---|---|
| **Embodied Energy (primary production)** | 80 | $E_p$ | [23] |
| **Secondary Production (recycled)** | 22 | $E_s$ | [23] |
| **Forming/Shaping Processes** | 20 | $E_f$ | |
| **Powder Atomization** | 34 | $E_a$ | [25] |
| **Conventional Machining** | Equation 6 | $E_{CM}$ | |
| **Metal Additive Forming** | Equation 10 | $E_{AM}$ | |
| **Hybrid Additive Subtractive** | Equation 15 | $E_{HM}$ | |

The embodied energy per kg ($E_{PS}$) to produce the parts from combination of recycled and primary sources can be estimated with Equation 1:

$$E_{PS} = E_p(1\text{-}r\%) + E_s r\% \quad (1)$$

Here, r% represents the percentage of recycled steel scrap used in the production process. Typically, percentage of recycled steel during production ranges from 35-40%. Total life cycle energy consumption per unit for a material stock of mass (m) in the case of conventional machining (CM) can be modeled with Equation 2:

$$E_{LC1} = m_{CM}(E_f + E_{PS}) + E_{CM} \quad (2)$$

Similarly, Equations 3 and 4 are used to model total life cycle energy per unit of mass $m_{AM}$ and $m_{HMss}$ in case of EBM and DMLS-HM respectively:

$$E_{LC2} = m_{AM}(E_a + E_{PS}) + E_{AM} \quad (3)$$

$$E_{LC3} = m_{HM}(E_a + E_{PS}) + E_{HM} \quad (4)$$

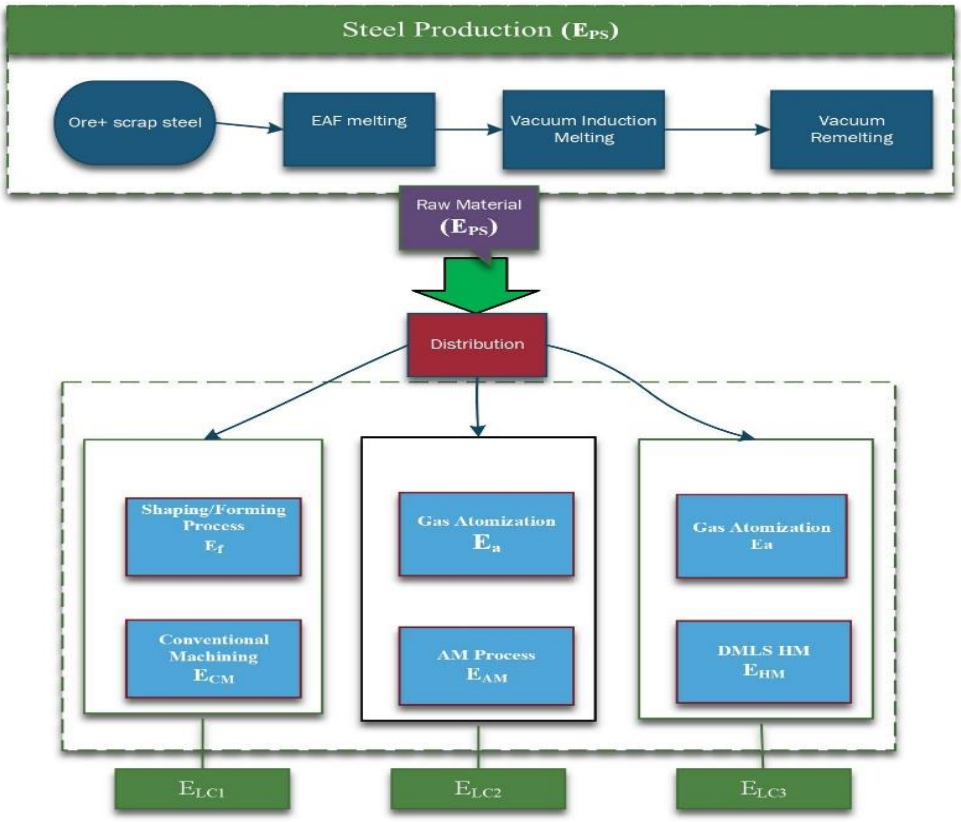


**Figure 18 Framework of Energy Model**

**Table 12 Geometry Dimensions and Features**

| | Geometry 1 | Geometry 2 | Geometry 3 |
|---|---|---|---|
| Solid-Envelope Ratio ($\alpha$) | 0.12 | 0.23 | 0.30 |
| CM stock mass (g) | 4000 | 4000 | 4000 |
| AM mass deposited (g) | 580 | 950 | 1300 |
| DMLS-HM deposited mass (g) | 700 | 970 | 1500 |
| Total volume ($mm^3$) | 62361.5 | 117715.5 | 151833.2 |
| Surface Area ($mm^2$) | 28253.7 | 28444.0 | 27595.8 |

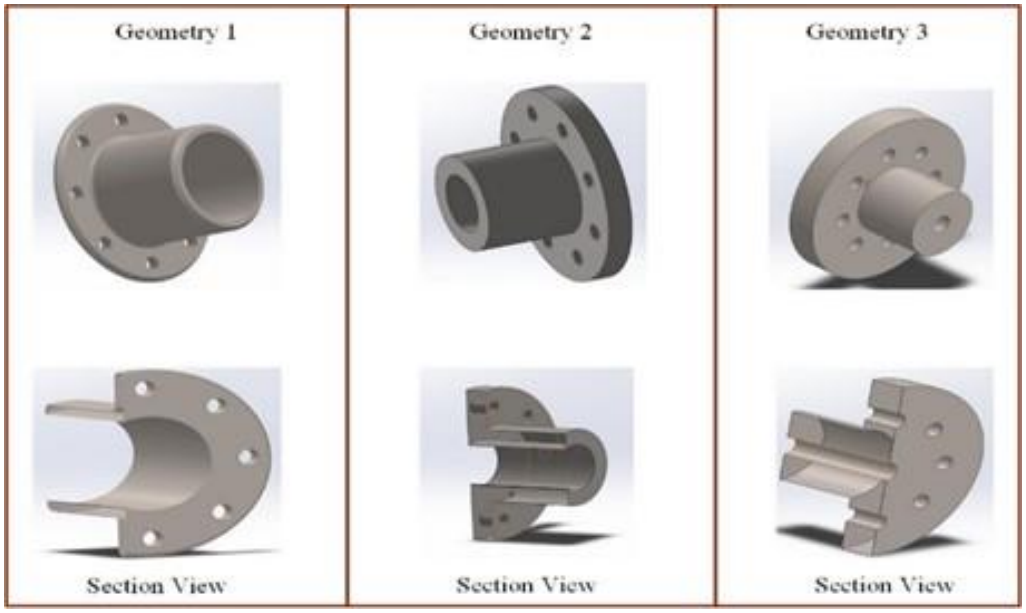


**Figure 19 Geometries and their Cross Sections**

Material lost during production of powder atomization process has been evaluated using the method used by Lavery et al. [67]. A yield value of 1.05representing the raw material used to produce 1 kg of metal powder.

The model of carbon emission from energy consumption proposed by Jeswiet and Kara [54] will be used to access the environmental impact of the three processes as shown in Equation 5.

$$\text{Carbon Emission} = CES^{TM}[\text{kg-CO2/MJ}] \times \text{Epart[MJ]} \quad (5)$$

$E_{part}$ is total energy requirements to manufacture the desired geometry and $CES^{TM}$ is carbon emission signature for energy. In the USA, an average 0.15 $CES^{TM}$ factor is used [68].

## 4.7 Conventional Machining

In conventional machining, milling refers to subtractive manufacturing process in which material is removed by a rotating multiple tooth cutter in the presence of cutting fluids to achieve the final surface. Mikron HSM 400 milling is used in energy estimation. Figure 20 shows the fuzzy values for power consumption during a typical machining process, note that tool maintenance is not considered in system boundary of this study.

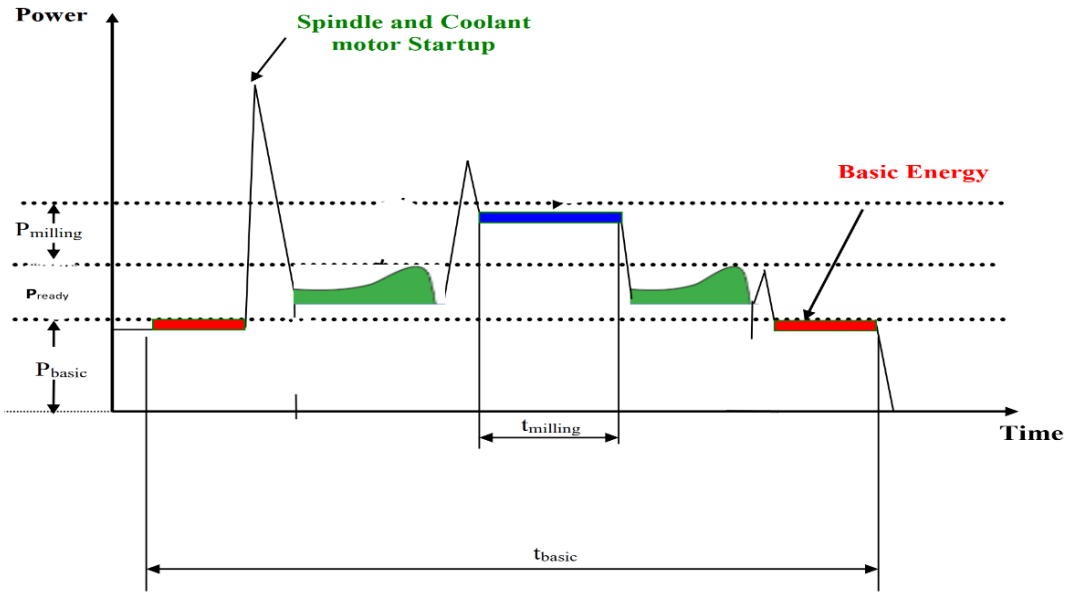


**Figure 20 Power Characteristic and Energy consumption in machine tool**

Gutowski et al.[42] provided the basis for energy requirements in machining operations and Mori et al.[45] expanded his work and introduced concept of idle power and basic power. Diaz et al. [43] found out that during machining operation, tool engages and disengages with material and modelled air cutting time that reduced the overestimation of energy demand. Balogun and Mativenga [41] further improved this model by incorporating works by Gutowski et al.[42], Mori et al.[45] and Diaz et al.[43] and developed an improved and robust model as shown in the Equation 6.

$$E_{CM} = P_b(t_b + t_r + t_c) + P_r(t_r) + P_{air}t_{air} + t_c(P_r + P_{cool} + P_{cutting}) \quad (6)$$

Here $P_b$ is basic power when machine is turned ON but without feed, cutting and spindle running and is only used to run auxiliary parts of machine such as computer, fan, motors etc. $P_b$ can be estimated experimentally by measuring constant energy consumption during the operation of auxiliary components. The $P_r$ is ready state power when machine is operating but not processing material such as power to bring tool close to cut position with workpiece and $P_{cool}$ is coolant power used to pump and circulate coolant during cutting. The $P_{air}$ is air cutting time when cutting tool is not engaged and retracting over the component. The k is specific cutting energy of material and $\dot{v}$ is material removal rate. The $t_{air}$ , $t_c$ , and $t_r$ represent air cut time, cutting time and ready state time

respectively and can be extracted from machine database. In Equation 6, $P_{b,}$ $P_{r,}$ $P_{air,}$ $P_{cool}$ are the constant components of a milling machine. Values of these constants were extracted from Mikron HSM 400 machine as reported by Balogun and Mativenga [41]. Cutting power mainly depends on cutting conditions such as feed rate $f_r$, axial (b) and radial depth of cut (d) and can be estimated using Equation 7.

$$P_{cutting} = CWk\dot{v} = (CWk)f_r bd \quad (7)$$

The value of k for stainless steel is 5 Ws/mm$^3$ and it is in the range reported by Kalpakjian and Schmid [69]. The value of k is affected by the interaction of cutting tool and workpiece material. The typical values of C and W, as reported by Walsh and Cormier [70] for stainless steel cutting conditions are 1.4 and 1.1 respectively. Equation 8 is used to estimate the theoretical cutting time of milling operation as follows:

$$t_{cut} = (L_f + A)/f_r \quad (8)$$

where A is distance to reach full cutter depth and $L_f$ is length of tool feed.

**Table 13 Cutting Parameters and Condition**

| Tool type | Coated Carbide tool |
|---|---|
| Feed per tooth(mm) | 0.06 |
| Cutting speed (m/min) | 60.32 |
| Cutter Diameter (mm) | 16 |
| Number of flutes | 4 |
| Spindle speed (rpm) | 1200 |
| Feed Rate (mm/min) | 288 |
| Axial depth of cut (mm) | 2.5 |
| Radial depth of cut (mm) | 2.5 |
| Environment Condition | Flood Coolant |

**Table 14 Energy Requirements Mikron HSM 400**

| | |
|---|---|
| Basic power (W) | 2904 |
| Ready power (W) | 401 |
| Tool change power (W) | 920 |
| Air cutting (W) | 2917 |
| Coolant power (W) | 1790 |

During milling operation, cutting fluids allow high speed cutting operations and prolong tool life. In CNC machine, cutting fluid pump circulates the fluid from cutting fluid tank to the cutting zone. Cutting fluid is recycled until it is disposed of after two weeks on average. Assuming a CNC with fluid tank capacity of 250 L pumps 210 hr./ 2 weeks, then the cutting fluid loss is 250L/ (210×60) per minute. The effective loss of cutting fluid due to degradation would be 0.02 L/min or about 20 g/min. The coolant is usually about 75 - 95 wt.% water. With 85wt% water, the coolant oil loss would be 3g cutting oil/min. Machine parameters such as cutting speed and feed as recommended by Kalpakjian and Schmid [69] and McCauley and Hoffman [71] have been shown in Table 13. Table 14 shows energy requirements for the machine.

## 4.8 Electron Beam Melting Additive Manufacturing

Electron beam melting (EBM) process has been employed in the energy framework. The energy consumption units in an EBM are shown in Fig. 21 and the energy requirements for the processes are listed on Table 15. Baumer et al. [50] found energy requirement using the following Equation 9 and 10.

$$E_{AM} = E_{startup} + E_{preheat} + E_{build} + E_{cooldown} \quad (9)$$

$$E_{AM} = P_{startup}t_{startup} + P_{preheat}t_{preheat} + P_{build}t_{build} + P_{cooldown}t_{cooldown} \quad (10)$$

Where $E_{startup}$, $E_{preheat}$, $E_{build,}$ and $E_{cooldown}$ are energy consumption during machine startup, preheating, material deposition and cooldown respectively. It is important to note that time for startup power and preheat is independent of part geometry and can be determined from machine database. $P_{build}$ and $t_{build}$ depends on machine parameters such as scanning speed (S), layer thickness ($l_h$), beam spot diameter (b) and hatch space being used. Zhang and Bernard [72] introduced theoretical framework to evaluate total build time in AM that takes real time of AM production into context in the estimation. So for a single part manufacturing per build, total build time can be calculated as:

$$T_{b1} = T_{mp} + T_{ls1} + T_{lp} + T_e \quad (11)$$

Where $T_{b1}$, $T_{mp}$, $Tl_{s1}$, $T_{lp}$ and $T_e$ in Equation 11 represent total build time, machine preparation time, total layer drawing time, layer preparation time and time for ending operations respectively. Typically, during AM process, machine preparation time and

ending operations remain fixed. Fractions of the total time such as $T_{lp1}$, $T_{ls1}$ for single part production can be calculated using Equations 12 and 13.

$$T_{lp1} = (Z_1/l_h)t_l \quad (12)$$

Where $Z_1$, $l_h$, and $t_l$ denote workpiece height, layer thickness and time for preparation of one layer respectively.

$$T_{ls1} = [V_n/l_h]/[N(d_l+d_h)S]+[A_n/l_h]/S \quad (13)$$

Where $V_n$, N, $d_l$, $d_h$, and $A_n$ represent volume of part, number of laser heads, laser diameter, hatching space and surface area respectively.

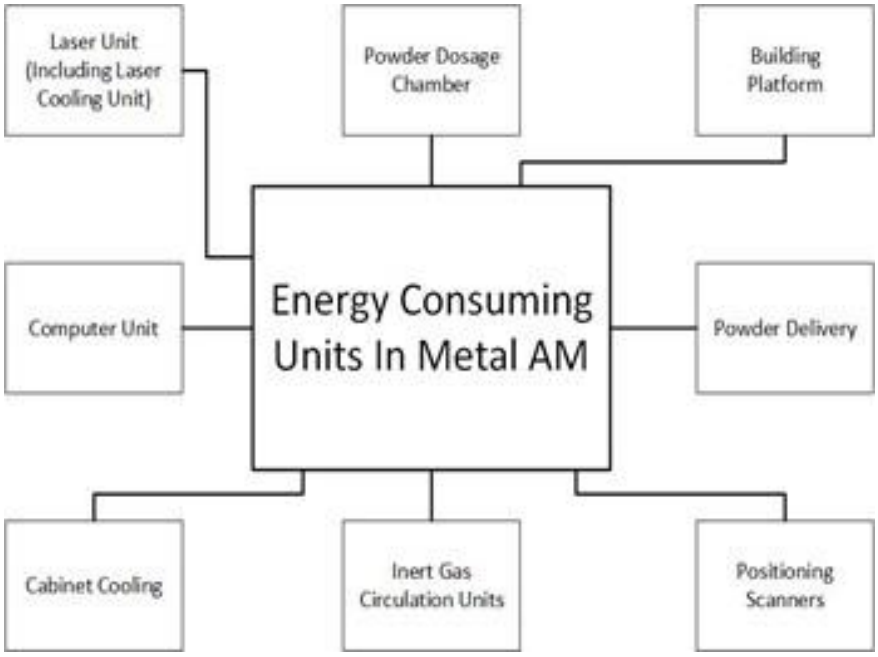


**Figure 21 Energy Consuming Units for EBM**

**Table 15 ARCAM A1 EBM Energy requirements**

| | |
|---|---|
| Machine startup (W) | 1090 |
| Preheating (W) | 3900 |
| Cool Down (W) | 600 |
| Building power (W) | 2220 |

## 4.9 Additive Subtractive (Hybrid) Machining

Since DMLS-HM is a robust combination of additive and subtractive process, theoretically, total energy consumption would be equal to energy consumed during additive process and subtractive process. To find total energy requirements, both additive and subtractive units have been subdivided into smaller units called energy consuming units (ECU). Figure 22 shows the major ECUs.

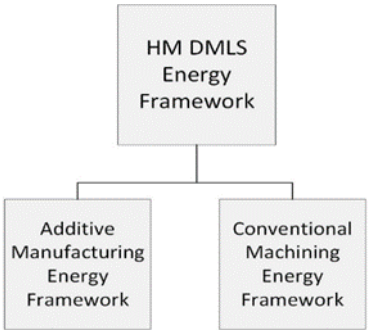


**Figure 22 DMLS-HM theoretical framework**

Basic physics and methodology of theoretical framework of additive and subtractive aligns with energy frameworks developed and employed by Jackson et al.[25] and Peng and Sen [52] for additive subsystems and Balogun and Mativenga [41] Gutowski et al. [42] for subtractive subsystem. Energy consumed in additive sub-unit of DMLS-HM can be calculated using following equation.

$$E_{DMLS} = P_{basic}(t_{squeezing}+t_{ready}) + t_{sintering}(P_{squeezing} + P_{inert}+P_{sintering}) \quad (14)$$

Since total energy requirements are combination of both additive and subtractive unit, combining equation [6] and [14] would give Equation 15

$$E_{HM}=P_{basic}(t_{squeezing}+t_{ready})+P_{air}t_{air}+ n_t(P_{tool}t_{tool})+ t_{sintering}(P_{squeezing}+P_{inert}+P_{sintering})+t_{cut}(P_{milling}+P_{coolant}+P_{basic}) \quad (15)$$

Where $P_{sintering}$ is power requirement during laser exposure, $P_{squeezing}$ represents power requirement for recoating of layer on build stage, $P_{basic}$ is machine basic background power for machine auxiliary components like computer, fans, driving motors. $P_{coolant}$ and $P_{inert}$ are power requirements to pump coolant and inert gas in chamber respectively. $n_t$ represents number of tool used. $P_{tool}$ represents tool change power and $P_{milling}$ is power

requirement during subtractive operation. Since these values depend on machine being used, power requirement values were extracted from LUMEX 25 DMLS-HM [73] machine data. Total cycle time ($t_{cycle}$) can be evaluated using Equation 16:

$$t_{cycle}=V/Q \quad (16)$$

Where Q is volumetric built rate and V is total volume of geometry. For surfaces with lower complexity, a typical range of cutting time is 30-35% [70] and cutting time increases depending on complexity of geometry and desired surface finish. Geometries under consideration are relatively small and simple. So, 30% of cycle time is allocated to milling. Table 16 and 17 show machine parameters and power requirements used in the study respectively.

**Table 16 Machine Parameters DMLS-HM**

| | |
|---|---|
| Q ($mm^3/h$) | 35000 |
| Scan speed (mm/s) | 300 |
| Beam diameter (mm) | 0.1 |

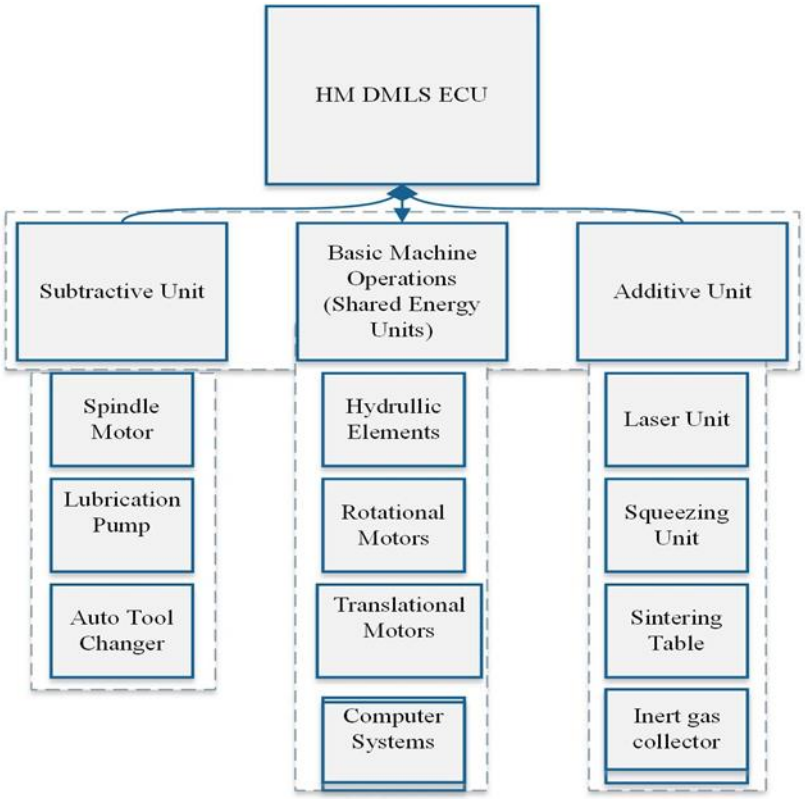


**Figure 23 DMLS-HM energy consuming units (ECU)**

**Table 17 Power requirements in DMLS-HM [73]**

| | |
|---|---|
| Air Cut (W) | 2917 |
| Coolant state Power (W) | 750 |
| Tool change power (W) | 200 |
| Basic state Power (W) | 28500 |
| Squeezing Power (W) | 400 |
| Ready State Power (W) | 2000 |
| Milling Power (W) | 100 |
| Inert gas system (W) | 3000 |
| Laser Power (W) | 320 |

# CHAPTER 5

# 5 ECO-IMPACT EVALUATION RESULTS AND DISCUSSION

## 5.1 Introduction

From chapter 4, equations 6,10 and 15 have been used to calculate the total energy requirements in conventional machining, electron beam melting and hybrid additive subtractive (DMLS-HM) manufacturing. The resulting energy values has been converted into equivalent carbon emission using methodology demonstrated by Jeswiet and Kara [54]. Bar graphs in result sections describe the relative performance with respect to energy consumption for all the three manufacturing techniques with fabrication of same geometry.

## 5.2 Results and Discussion

The total energy consumption from cradle-to-gate for the conventional machining process for geometry 1 with solid-envelope ratio of 0.12 shown in Figure 24 is 327.1MJ/unit which is highest when compared to 75.8 MJ/unit for EBM and 204.4 MJ/unit for DMLS-HM. This can be attributed to the stock requirement for CM to produce 580g geometry; about 87% of the stock material was wasted in form of chips. However, in the cases of DMLS-HM and EBM processes, material requirement is relatively lower for the final part because both processes form their geometries by building the metal alloy layer by layer with very little waste. Though, DMLS-HM has a subtractive unit integrated with the machine system, its primary purpose is to conduct finish-operation on the geometry which in turn generates very low amount of chips. Moreover, material requirement may be high in case of CM, but material processing (machining) energy is relatively lower than for EBM and DMLS-HM.

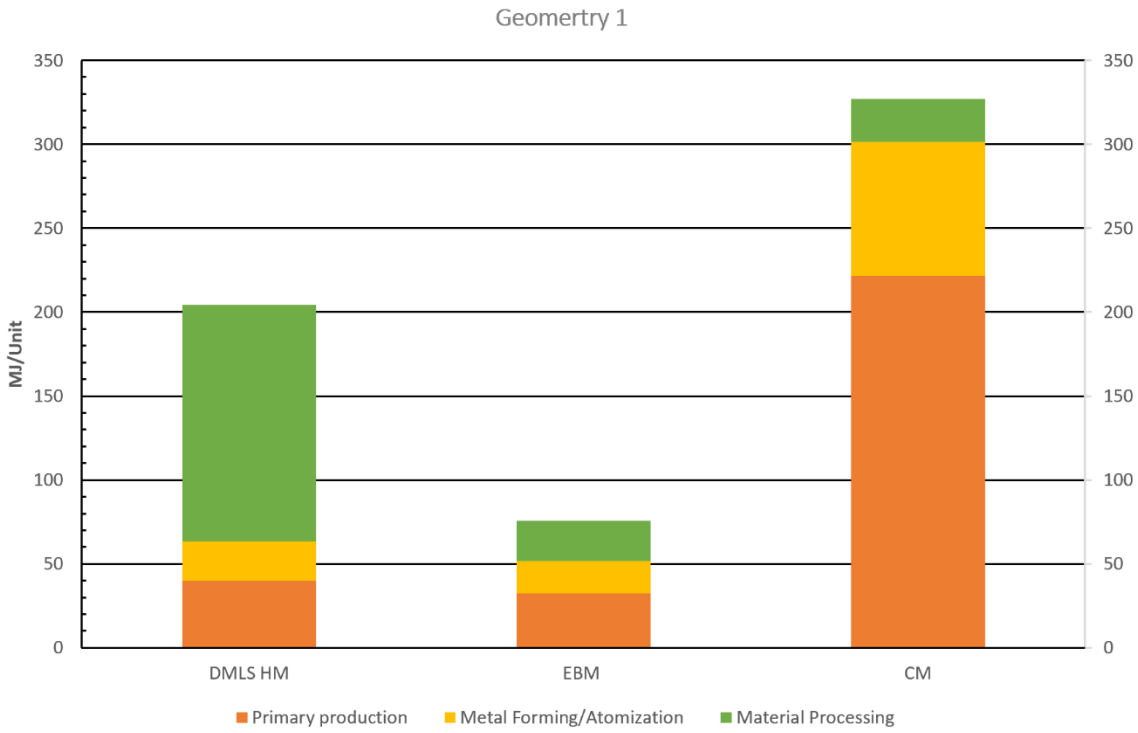


**Figure 24 Energy Consumption for Geometry 1, $\alpha$ is 0.12**

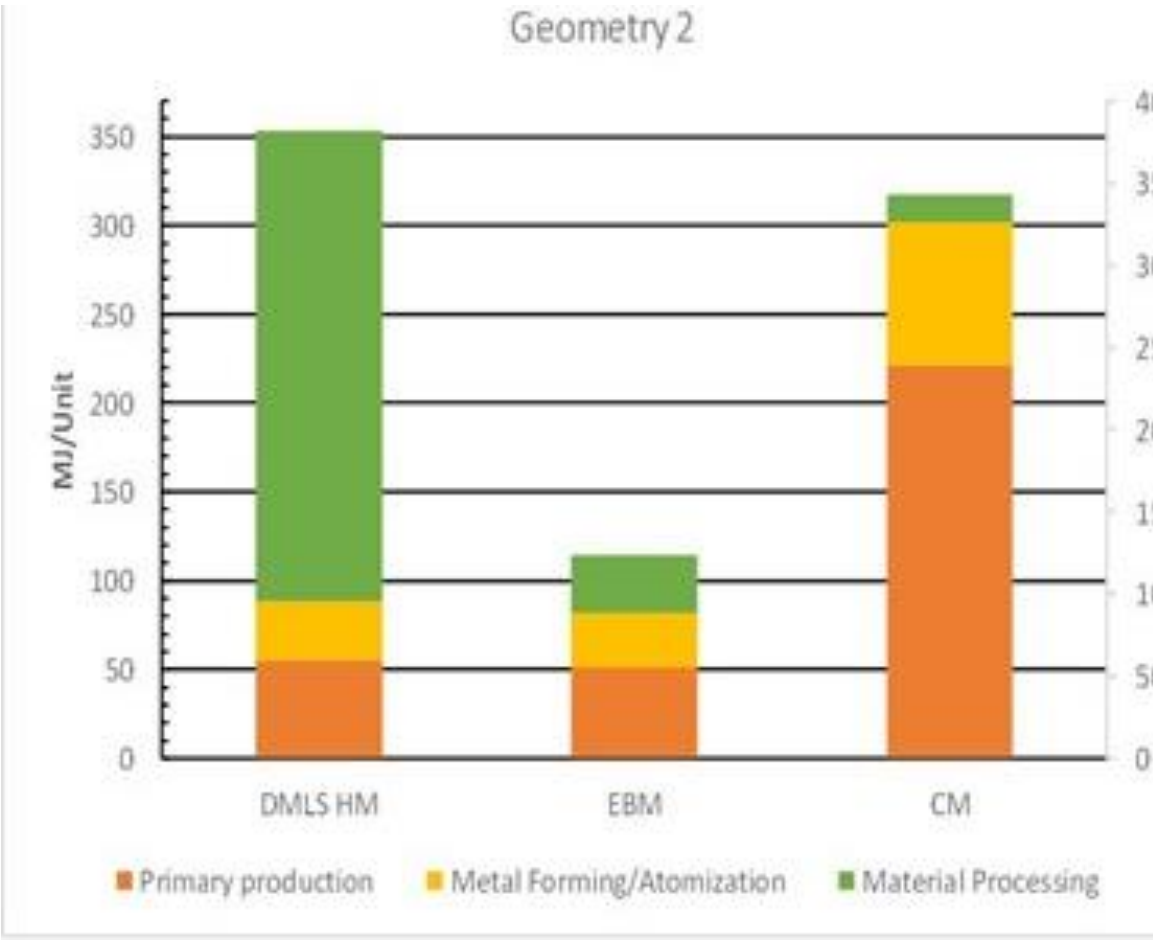


**Figure 25 Energy consumption for Geometry 2, α is 0.23**

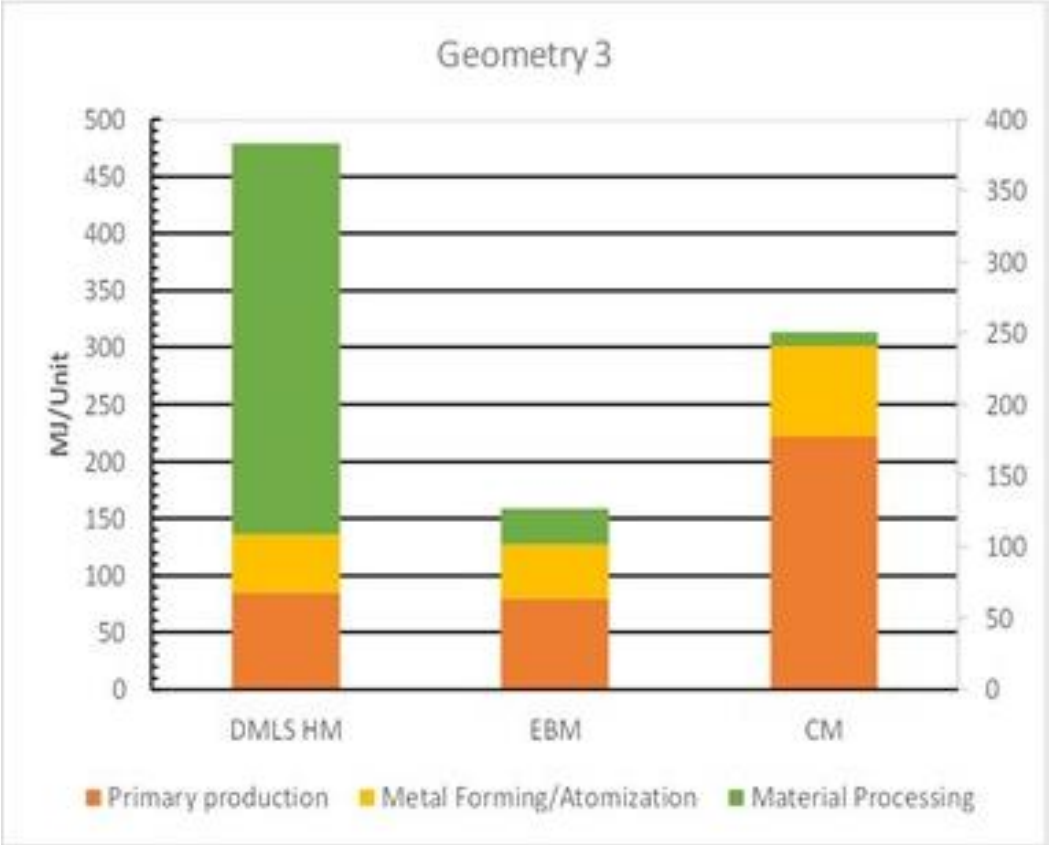


**Figure 26 Energy consumption for Geometry 3, α is 0.30**

For geometries 2 and 3 with α of 0.23 and 0.30 respectively, total energy consumption is highest in case of DMLS-HM as shown in Figures 25 and 26 respectively. To produce a part with high volume and large number of layers, EBM required relatively more time for material processing that led to increase in the energy requirements. However, the material requirement was relatively lower than for conventional machining process. The total energy requirements for geometries 2 and 3 for EBM process were 114.3 MJ/unit and 159.1 MJ/unit as compared to 317.5 MJ/unit and 313.7 MJ/unit for CM. As expected, energy requirements in case of CM for geometries 2 and 3 were lower than for geometry 1. This is because geometry 1 required high machining time due to the large cavity feature. But with increased solid to envelope ratio, final geometry was close to stock material and resulting machining time reduced accordingly. The solid-to-envelope ratio, α has more effect on the energy model of the additive processes (DMLS-HM and EBM) than it does on the subtractive machining (CM) process. The average percentage change

in $\alpha$ resulted to equal percentage change in energy consumption of DMLS-HM and EBM. It had no significant effect on the energy consumption model of the CM process with about 1.5% average change in the energy consumption compared to the major changes in $\alpha$. The CM process showed dominant energy consumption during the primary production stage with an average 70% more than EBM and DMLS-HM processes. However, the DMLS-HM was dominant in energy consumption during the shape forming production stage with an average 89% more energy consumption than CM and EBM processes. It is important to note that energy requirements can be varied depending on machine parameters used. It can be deduced from theoretical energy frameworks that energy consumption is highly influenced by the machine parameters used. In addition, auxiliary components of machine also play an important role. For example, two hybrid DMLS HM operating at the same parameters may have different energy requirements depending on the power requirements of its fans, computers, air compressor etc and working condition of machine.

When $\alpha$ is 0.12, EBM presented lowest energy consumption in the shape forming stage of the production with average of 80% lower energy than DMLS-HM and 2% lower than CM. The EBM's low energy is attributed to its high process rate. It has been established that energy consumption in AM is influenced by the process rate and that energy efficiency in AM can be improved by increasing process rates [22]. The heat transfer mechanisms required to deliver the melt stream to build a part in AM limits the process rate level that can be achieved. However, due diligence should be paid to avoid sacrificing build quality with too high process rate. The specific energy consumed in CM process is also highly dependent on the rate of material removal [41]. The finish-machining conducted after fusion of successive ten layers of stainless steel 316L powder will result in additional specific energy consumption by the DMLS-HM process. This explains the higher specific energy consumption during the rough machining with small material removal rate in the CM process. To maintain longer tool life and reasonable parts' surface finish, the rate of material removal needs to be lower than the EBM process. As a result, the EBM process tend to consume less energy than the CM and DMLS-HM processes as shown in Figures 24, 25, and 26.

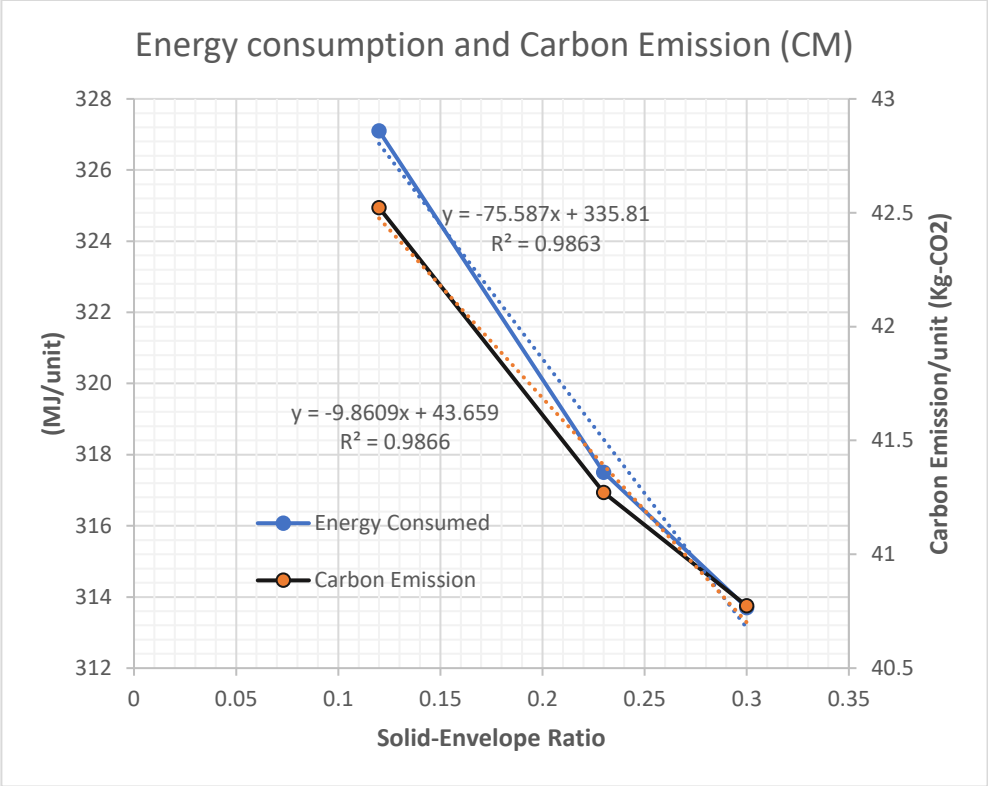


**Figure 27 Effect of solid-to-envelope ratio, α on energy and carbon emission of conventional machining**

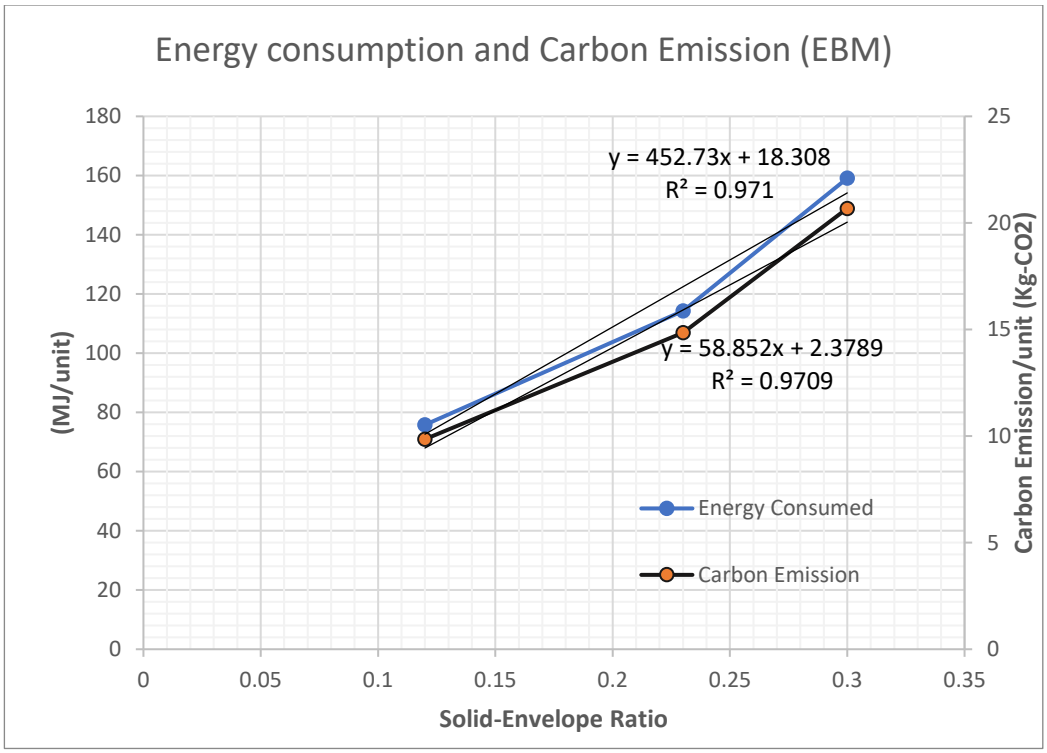


**Figure 28 Effect of solid-to-envelope ratio, $\alpha$ on energy and carbon emission of electron beam melting**

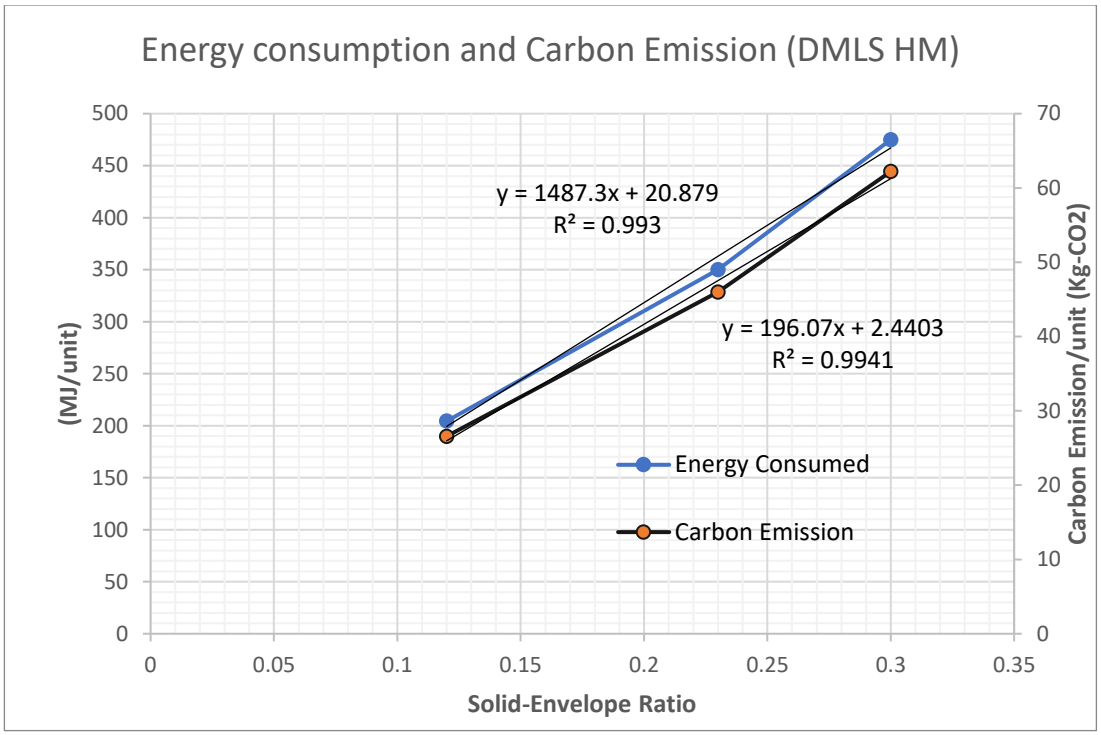


**Figure 29 Effect of solid-to-envelope ratio on energy and carbon emission of DMLS-HMnd carbon emission of electron beam melting**

The effect of solid-to-envelope ratio, α on energy consumption and carbon emission of the three processes CM, EBM, and DMLS-HM are shown in Figures 27, 28, and 29 respectively. The solid-to-envelope ratio has statistically significant effect on energy consumption and carbon emission without sign of interaction effect between them. Evaluation of total energy consumption and carbon emission of the processes showed that DMLS-HM had highest carbon emission during the cradle-to-gate production phases with an average of 80% more than EBM and CM processes. The CM was dominant in the carbon emission during the primary production stage with an average of 70% more energy than DMLS-HM and EBM processes. There exists very strong correlation between the performance measurements (energy consumption and carbon emission) and solid-to-envelope, α and this can be useful in design phase to optimize product design for sustainable manufacturing.

**Table 18 Energy Consumption during Fabrication of Materials Using AM process**

| Machine | Process | Material | Specific Energy Consumption (MJ/kg) | Resource Consumption | Reference |
|---|---|---|---|---|---|
| MTT SLM250 | SLM | SS 316L | 112-140 | n/a | [49] |
| MTT SLM251 | SLM | SS 316L | 83-108 | n/a | |
| CONCEPT LASER M3 LINEAR | SLM | SS 316L | 423-588 | n/a | [17] |
| CONCEPT LASER M3 LINEAR | SLM | SS 316L | 96.8 | Nitrogen: 3.5m³/h 20.4% waste powder | [74] |
| Arcam A1 | EBM | Ti-6Al-4V | 60 | 1 L/h Helium | [50] |
| Arcam A1 | EBM | Ti-6Al-4V | 61.0-177.0 | n/a | [17] |
| Arcam | EBM | Ti-6Al-4V | 375 | Argon gas: 5.5m³/h | [75] |

Table 18 shows that in published literature SEC for SS 316L lies within range of 83-140 MJ/kg when processed through selective laser melting. Baumer et al. [17] reported higher energy consumption per kilogram of material deposited and lower process rates values. SEC is also influenced by capacity utilization of built table as reported by Liu et al. [18].It is possible that SEC for [17]is higher because of poor utilization.

In a typical manufacturing operation, built rate of EBM is kept higher than SLM. So, if SS 316L is to be processed using EBM process for relatively low solid-envelope ratio, it is expected that SEC for material processing (ignoring embedded energy EPS) values would lie in the range of 20-40 MJ/kg as calculated by theoretical framework. Because of high specific heat ( 0.5263 J/g-°C) of Ti-6Al-4V, more energy is required to melt the same amount of SS 316L (0.26 J/g-°C) material. No published data on the processing of SS 316L using EBM and DMLS HM was found.

## 5.3 Conclusion

Analytical model of energy consumption for direct metal laser sintering hybrid milling (DMLS-HM) process was developed and used to evaluate total energy consumed during manufacture of stainless steel 316L parts of different solid-to-envelope ratio, $\alpha$. The cradle-to-gate life cycle inventory (LCI) of the DMLS-HM was compared to those of conventional machining and electron beam melting (EBM) used to produce the same part geometries. It was found that $\alpha$ will have more impact on the energy model of the additive processes than on the subtractive machining process. On average, the percentage change in $\alpha$ is equal to the percentage change in energy consumption and carbon emission of DMLS-HM and EBM. The CM process had little average change of 1.5% compared to the major changes in $\alpha$. The DMLS-HM process shows dominant energy consumption during the primary production stage with an average 84% more than EBM and CM processes. However, the CM was dominant in energy consumption during the shape forming production stage with an average 70% more energy than DMLS-HM and EBM processes. The energy and carbon emission values estimated with the developed analytical models were not verified empirically but are within the range of reported data in the literature for the processes considered.

# CHAPTER 6

# 6 CONCLUSIONS AND FUTURE WORK

## 6.1 Impact of Research

- This study has provided a standard approach of comparison and better understanding the metallurgical and mechanical properties of geometries produced by DMLS-HM and DMLS. Moreover, this will assist in assessment of process structure and property relationships which in turn will provide a roadmap for design and manufacture of customized properties.

- This research provided further insights into sustainable viewpoint of AM and summarized its performance compared to conventional subtractive operations, AM is relatively less wasteful. Also, study provides a systemic approach that will enable the identification of ecologically friendly process selection.
- This work provides analytical framework to comprehensively analyze and compare the feasibility of manufacturing processes based on overall energy consumption. For example, for lower solid to envelop ratios, additive manufacturing process is more energy efficient as there will be lower number of horizontal slices to build. However, for larger solid-envelope ratios. conventional subtractive processes will be more feasible considering the stock material would be closer to final geometry and less material will be removed
- This thesis further substantiates the notion that one cannot categorically argue that any single manufacturing approach is the more efficient than others. Rather, it largely depends on volume of geometry to be removed or deposited, processing time and process variables.

## 6.2 Future Work

- Fatigue testing would help understanding the relative performance. Fatigue tests will explain how as-built and age-hardened samples of DMLS- would behave under cyclic loading.
- Non-destructive testing (ultrasound testing, magnetic flux leakage etc.) to evaluate electrical properties and internal defects.
- Energy consumption results were compared and validated with published literature. Further research is needed to further validate experimental studies as well as make iterative improvements in energy consumption frameworks
- This thesis carried out sustainability analysis using LCA principles; however, potential environmental toxicity during material handling, transportation of material within machine shop, disposal of waste material and product use has been ignored. Moreover, input resources such as chemical solvents, emissions of

aerosol has been overlooked assuming their insignificance .There is a need of comprehensive investigation with respect to environmental performance evaluation that covers all aspects of product life cycle from procurement of raw material to final disposal (cradle to grave).

- This research study was limited to environmental sustainability and did not deal with the economic or social sustainability. A more balanced and comprehensive research study on cost-benefit analysis and its significance in supply chains relative to conventional DMLS or EBM machine.
- A thorough environmental impact assessment is contingent upon quality of LCI. LCI of AM and DMLS-HM mainly covered input energy and input material resources and ignored inert gases (used to prevent melting powder from oxidation) and other consumables because of low quality of LCI data present in literatures or no data was available. Moreover, assessment describing the environmental impact indicators such as acidification, eutrophication, human toxicity, ecotoxicity have not been discussed. LCI coupled with a standard life cycle impact assessment (LCIA) such as ReCiPe would further delineate the aspects of sustainability.

# 7 REFERENCES


[1] F42 Committee, "Terminology for Additive Manufacturing Technologies," ASTM International, West Conshohocken,PA, 2012.

[2] L. W. Weber *et al.*, "The Role of the National Science Foundation in the Origin and Evolution of Additive Manufacturing in the United States." 2013.

[3] B. Berman, "3-D printing: The new industrial revolution," *Business Horizons*, vol. 55, no. 2, pp. 155–162, Mar. 2012.

[4] M. Attaran, "The rise of 3-D printing: The advantages of additive manufacturing over traditional manufacturing," *Business Horizons*, vol. 60, no. 5, pp. 677–688, Sep. 2017.

[5] W. Gao *et al.*, "The status, challenges, and future of additive manufacturing in engineering," *Computer-Aided Design*, vol. 69, pp. 65–89, Dec. 2015.

[6] "ASTM F2792 - 12a Standard Terminology for Additive Manufacturing Technologies, (Withdrawn 2015)." [Online]. Available: https://www.astm.org/Standards/F2792.htm. [Accessed: 23-May-2019].

[7] "Directed Energy Deposition 3D Printing Service - Wire Fed and Powder..." [Online]. Available: https://www.3diligent.com/3d-printing-service/directed-energy-deposition/. [Accessed: 23-May-2019].
[8] X. Wang, M. Jiang, Z. Zhou, J. Gou, and D. Hui, "3D printing of polymer matrix composites: A review and prospective," *Composites Part B: Engineering*, vol. 110, pp. 442–458, Feb. 2017.
[9] T. D. Ngo, A. Kashani, G. Imbalzano, K. T. Q. Nguyen, and D. Hui, "Additive manufacturing (3D printing): A review of materials, methods, applications and challenges," *Composites Part B: Engineering*, vol. 143, pp. 172–196, Jun. 2018.
[10] W. R. Morrow, H. Qi, I. Kim, J. Mazumder, and S. J. Skerlos, "Environmental aspects of laser-based and conventional tool and die manufacturing," *Journal of Cleaner Production*, vol. 15, no. 10, pp. 932–943, Jan. 2007.
[11] M. Baumers, C. Tuck, D. L. Bourell, R. Sreenivasan, and R. Hague, "Sustainability of additive manufacturing: measuring the energy consumption of the laser sintering process," *Proceedings of the Institution of Mechanical Engineers, Part B: Journal of Engineering Manufacture*, vol. 225, no. 12, pp. 2228–2239, Dec. 2011.
[12] H.-S. Yoon *et al.*, "A comparison of energy consumption in bulk forming, subtractive, and additive processes: Review and case study," *International Journal of Precision Engineering and Manufacturing-Green Technology*, vol. 1, no. 3, pp. 261–279, Jul. 2014.
[13] J. Faludi, C. Bayley, S. Bhogal, and M. Iribarne, "Comparing environmental impacts of additive manufacturing vs traditional machining via life-cycle assessment," *Rapid Prototyping Journal*, vol. 21, no. 1, pp. 14–33, Jan. 2015.
[14] C. Telenko and C. Conner Seepersad, "A comparison of the energy efficiency of selective laser sintering and injection molding of nylon parts," *Rapid Prototyping Journal*, vol. 18, no. 6, pp. 472–481, Sep. 2012.
[15] K. Kellens, R. Renaldi, W. Dewulf, J. Kruth, and J. R. Duflou, "Environmental impact modeling of selective laser sintering processes," *Rapid Prototyping Journal*, vol. 20, no. 6, pp. 459–470, Oct. 2014.
[16] F. L. Bourhis, O. Kerbrat, J.-Y. Hascoet, and P. Mognol, "Sustainable manufacturing: evaluation and modeling of environmental impacts in additive manufacturing," *Int J Adv Manuf Technol*, vol. 69, no. 9, pp. 1927–1939, Dec. 2013.
[17] M. Baumers, C. Tuck, R. Wildman, I. Ashcroft, and R. Hague, "Energy Inputs to Additive Manufacturing Does Capacity Utilization - Technische Informationsbibliothek (TIB)," in *SOLID FREEFORM FABRICATION PROCEEDINGS*, Austin, 2011, p. 11.
[18] Z. Y. Liu, C. Li, X. Y. Fang, and Y. B. Guo, "Energy Consumption in Additive Manufacturing of Metal Parts," *Procedia Manufacturing*, vol. 26, pp. 834–845, Jan. 2018.
[19] E. Braastad, "Energy Consumption of a Hybrid Additive-Subractive Manufacturing Process," p. 96.
[20] D. L. Bourell, D. W. Rosen, and M. C. Leu, "The Roadmap for Additive Manufacturing and Its Impact," *3D Printing and Additive Manufacturing*, vol. 1, no. 1, pp. 6–9, Mar. 2014.
[21] M. Kafara, M. Süchting, J. Kemnitzer, H.-H. Westermann, and R. Steinhilper, "Comparative Life Cycle Assessment of Conventional and Additive Manufacturing

in Mold Core Making for CFRP Production," *Procedia Manufacturing*, vol. 8, pp. 223–230, Jan. 2017.
[22] N. Emami *et al.*, "A Life Cycle Assessment of Two Residential Buildings Using Two Different LCA Database-Software Combinations: Recognizing Uniformities and Inconsistencies," *Buildings*, vol. 9, no. 1, p. 20, Jan. 2019.
[23] M. Ashby, *Materials and the Environment - 2nd Edition*, 2nd ed. Michael Ashby, 2012.
[24] W. Du, Q. Bai, and B. Zhang, "A Novel Method for Additive/Subtractive Hybrid Manufacturing of Metallic Parts," *Procedia Manufacturing*, vol. 5, pp. 1018–1030, 2016.
[25] M. A. Jackson, A. Van Asten, J. D. Morrow, S. Min, and F. E. Pfefferkorn, "Energy Consumption Model for Additive-Subtractive Manufacturing Processes with Case Study," *International Journal of Precision Engineering and Manufacturing-Green Technology*, vol. 5, no. 4, pp. 459–466, Aug. 2018.
[26] X. C. Wang, T. Laoui, J. Bonse, J. P. Kruth, B. Lauwers, and L. Froyen, "Direct Selective Laser Sintering of Hard Metal Powders: Experimental Study and Simulation," *The International Journal of Advanced Manufacturing Technology*, vol. 19, no. 5, pp. 351–357, Mar. 2002.
[27] S. Rossi, F. Deflorian, and F. Venturini, "Improvement of surface finishing and corrosion resistance of prototypes produced by direct metal laser sintering," *Journal of Materials Processing Technology*, vol. 148, no. 3, pp. 301–309, May 2004.
[28] J. Kruth, P. Mercelis, J. Van Vaerenbergh, L. Froyen, and M. Rombouts, "Binding mechanisms in selective laser sintering and selective laser melting," *Rapid Prototyping Journal*, vol. 11, no. 1, pp. 26–36, Feb. 2005.
[29] G. Casalino, S. L. Campanelli, N. Contuzzi, and A. D. Ludovico, "Experimental investigation and statistical optimisation of the selective laser melting process of a maraging steel," *Optics & Laser Technology*, vol. 65, pp. 151–158, Jan. 2015.
[30] C. Tan *et al.*, "Microstructure and Mechanical Properties of 18Ni-300 Maraging Steel Fabricated by Selective Laser Melting," in *Proceedings of the 2016 6th International Conference on Advanced Design and Manufacturing Engineering (ICADME 2016)*, Zhuhai, Indonesia, 2016.
[31] A. G. Demir and B. Previtali, "Investigation of remelting and preheating in SLM of 18Ni300 maraging steel as corrective and preventive measures for porosity reduction," *Int J Adv Manuf Technol*, vol. 93, no. 5, pp. 2697–2709, Nov. 2017.
[32] S. R. Pogson, P. Fox, C. J. Sutcliffe, and W. O'Neill, "The production of copper parts using DMLR," *Rapid Prototyping Journal*, vol. 9, no. 5, pp. 334–343, Dec. 2003.
[33] H. H. Zhu, J. Y. H. Fuh, and L. Lu, "Microstructural evolution in direct laser sintering of Cu-based metal powder," *Rapid Prototyping Journal*, vol. 11, no. 2, pp. 74–81, Apr. 2005.
[34] X. Wang, M. Wraith, S. Burke, H. Rathbun, and K. DeVlugt, "Densification of W–Ni–Fe powders using laser sintering," *International Journal of Refractory Metals and Hard Materials*, vol. 56, pp. 145–150, Apr. 2016.
[35] K. V. Rajkumar *et al.*, "Characterization of aging behaviour in M250 grade maraging steel using eddy current non-destructive methodology," *Materials Science and Engineering: A*, vol. 464, no. 1–2, pp. 233–240, Aug. 2007.

[36] R. Casati, J. Lemke, A. Tuissi, and M. Vedani, “Aging Behaviour and Mechanical Performance of 18-Ni 300 Steel Processed by Selective Laser Melting,” *Metals*, vol. 6, no. 9, p. 218, Sep. 2016.
[37] J. Suryawanshi, K. G. Prashanth, and U. Ramamurty, “Tensile, fracture, and fatigue crack growth properties of a 3D printed maraging steel through selective laser melting,” *Journal of Alloys and Compounds*, vol. 725, pp. 355–364, Nov. 2017.
[38] H. Azizi *et al.*, “Metallurgical and mechanical assessment of hybrid additively-manufactured maraging tool steels via selective laser melting,” *Additive Manufacturing*, vol. 27, pp. 389–397, May 2019.
[39] T. Bhardwaj and M. Shukla, “Effect of laser scanning strategies on texture, physical and mechanical properties of laser sintered maraging steel,” *Materials Science and Engineering: A*, vol. 734, pp. 102–109, Sep. 2018.
[40] CO2PE Group, “CO2PE.” [Online]. Available: https://www.co2pe.org/?Taxonomy. [Accessed: 27-May-2019].
[41] V. A. Balogun and P. T. Mativenga, “Modelling of direct energy requirements in mechanical machining processes,” *Journal of Cleaner Production*, vol. 41, pp. 179–186, Feb. 2013.
[42] T. Gutowski, J. Dahmus, and A. Thiriez, “Electrical Energy Requirements for Manufacturing Processes,” p. 5, 2006.
[43] N. Diaz, M. Helu, A. Jarvis, S. Tönissen, D. Dornfeld, and R. Schlosser, “Strategies for Minimum Energy Operation for Precision Machining,” Jul. 2009.
[44] Y. He, F. Liu, T. Wu, F.-P. Zhong, and B. Peng, “Analysis and estimation of energy consumption for numerical control machining,” *Proceedings of the Institution of Mechanical Engineers, Part B: Journal of Engineering Manufacture*, vol. 226, no. 2, pp. 255–266, Feb. 2012.
[45] M. Mori, M. Fujishima, Y. Inamasu, and Y. Oda, “A study on energy efficiency improvement for machine tools,” *CIRP Annals*, vol. 60, no. 1, pp. 145–148, 2011.
[46] A. A. Munoz and P. Sheng, “An analytical approach for determining the environmental impact of machining processes,” *Journal of Materials Processing Technology*, vol. 53, no. 3, pp. 736–758, Sep. 1995.
[47] G. Ingarao, P. C. Priarone, F. Gagliardi, R. Di Lorenzo, and L. Settineri, “Subtractive versus mass conserving metal shaping technologies: an environmental impact comparison,” *Journal of Cleaner Production*, vol. 87, pp. 862–873, Jan. 2015.
[48] S. Ford and M. Despeisse, “Additive manufacturing and sustainability: an exploratory study of the advantages and challenges,” *Journal of Cleaner Production*, vol. 137, pp. 1573–1587, Nov. 2016.
[49] M. Baumers, C. Tuck, R. Hague, I. Ashcroft, and R. Wildman, “A COMPARATIVE STUDY OF METALLIC ADDITIVE MANUFACTURING POWER CONSUMPTION,” pp. 278–288, 2010.
[50] M. Baumers, C. Tuck, R. Wildman, I. Ashcroft, and R. Hague, “Shape Complexity and Process Energy Consumption in Electron Beam Melting: A Case of Something for Nothing in Additive Manufacturing?,” *Journal of Industrial Ecology*, vol. 21, no. S1, pp. S157–S167, 2017.
[51] P. Mognol, D. Lepicart, and N. Perry, “Rapid prototyping: energy and environment in the spotlight,” *Rapid Prototyping Journal*, vol. 12, no. 1, pp. 26–34, Jan. 2006.

[52] T. Peng and W. Sun, “Energy modelling for FDM 3D printing from a life cycle perspective,” p. 16.
[53] O. US EPA, “Sources of Greenhouse Gas Emissions,” *US EPA*, 29-Dec-2015. [Online]. Available: https://www.epa.gov/ghgemissions/sources-greenhouse-gas-emissions. [Accessed: 29-May-2019].
[54] J. Jeswiet and S. Kara, “Carbon emissions and CES$^{TM}$ in manufacturing,” *CIRP Annals*, vol. 57, no. 1, pp. 17–20, Jan. 2008.
[55] M. Gebler, A. J. M. Schoot Uiterkamp, and C. Visser, “A global sustainability perspective on 3D printing technologies,” *Energy Policy*, vol. 74, pp. 158–167, Nov. 2014.
[56] T. Peng, “Analysis of Energy Utilization in 3D Printing Processes,” *Procedia CIRP*, vol. 40, pp. 62–67, 2016.
[57] H. P. N. Nagarajan and K. R. Haapala, “Environmental Performance Evaluation of Direct Metal Laser Sintering through Exergy Analysis,” *Procedia Manufacturing*, vol. 10, pp. 957–967, Jan. 2017.
[58] RENISHAW, “Maraging steel M300 (H-5800-3695) powder for additive manufacturing.” RENISHAW INC, 2017.
[59] E28 Committee, “Test Methods for Tension Testing of Metallic Materials,” ASTM International.
[60] E28 Committee, “Test Methods for Rockwell Hardness of Metallic Materials,” ASTM International.
[61] E28 Committee, “Test Methods for Notched Bar Impact Testing of Metallic Materials,” ASTM International.
[62] K. Kempen, E. Yasa, L. Thijs, J.-P. Kruth, and J. Van Humbeeck, “Microstructure and mechanical properties of Selective Laser Melted 18Ni-300 steel,” *Physics Procedia*, vol. 12, pp. 255–263, 2011.
[63] Y. Bai, Y. Yang, D. Wang, and M. Zhang, “Influence mechanism of parameters process and mechanical properties evolution mechanism of maraging steel 300 by selective laser melting,” *Materials Science and Engineering: A*, vol. 703, pp. 116–123, Aug. 2017.
[64] E. Yasa, J. Deckers, J.-P. Kruth, M. Rombouts, and J. Luyten, “Charpy impact testing of metallic selective laser melting parts,” *Virtual and Physical Prototyping*, vol. 5, no. 2, pp. 89–98, Jun. 2010.
[65] A. Takano, S. Winter, M. Hughes, and L. Linkosalmi, “Comparison of life cycle assessment databases: A case study on building assessment,” *Building and Environment*, vol. 79, pp. 20–30, Sep. 2014.
[66] J. K. Watson and K. M. B. Taminger, “A decision-support model for selecting additive manufacturing versus subtractive manufacturing based on energy consumption,” *Journal of Cleaner Production*, vol. 176, pp. 1316–1322, Mar. 2018.
[67] N. P. Lavery, D. J. Jarvis, S. G. R. Brown, N. J. Adkins, and B. P. Wilson, “Life cycle assessment of sponge nickel produced by gas atomisation for use in industrial hydrogenation catalysis applications,” *Int J Life Cycle Assess*, vol. 18, no. 2, pp. 362–376, Feb. 2013.
[68] O. US EPA, “Global Greenhouse Gas Emissions Data,” *US EPA*, 12-Jan-2016. [Online]. Available: https://www.epa.gov/ghgemissions/global-greenhouse-gas-emissions-data. [Accessed: 11-Jan-2019].

[69] S. Kalpakjian and S. Schmid, *Manufacturing Engineering & Technology, 7th Edition*, 7th ed. Pearson, 2014.
[70] D. Cormier and R. A. Walsh, *McGraw-Hill Machining and Metalworking Handbook*, 3rd ed. 2005.
[71] C. J. McCauley and E. G. Hoffman, *Shop Reference for Students & Apprentices by Christopher J. McCauley and Edward G. Hoffman - Industrial Press eBookstore*, 2nd ed. Industrial Press, Inc., 2001.
[72] Y. Zhang and A. Bernard, "Generic build time estimation model for parts produced by SLS," in *High Value Manufacturing: Advanced Research in Virtual and Rapid Prototyping*, P. da Silva Bártolo, A. de Lemos, A. Pereira, A. Mateus, C. Ramos, C. Santos, D. Oliveira, E. Pinto, F. Craveiro, H. da Rocha Terreiro Galha Bártolo, H. de Amorim Almeia, I. Sousa, J. Matias, L. Durão, M. Gaspar, N. Fernandes Alves, P. Carreira, T. Ferreira, and T. Marques, Eds. CRC Press, 2013, pp. 43–48.
[73] "Matsuura Machinery Corporation | LUMEX Avance-25," *LUMEX series*, 04-Apr-2018. [Online]. Available: https://www.lumex-matsuura.com/english/contents/lumex25.html. [Accessed: 26-Apr-2019].
[74] K. Kellens, E. Yasa, W. Dewulf, J. P. Kruth, J. R. Duflou, and K. U. Leuven, "ENERGY AND RESOURCE EFFICIENCY OF SLS/SLM PROCESSES," presented at the International Solid Freeform Fabrication Symposium, 2011, p. 16.
[75] H. Paris, H. Mokhtarian, E. Coatanéa, M. Museau, and I. F. Ituarte, "Comparative environmental impacts of additive and subtractive manufacturing technologies," *CIRP Annals*, vol. 65, no. 1, pp. 29–32, 2016.